AD-A145 149 AERODYNAMICS OF AIRFOILS SUBJECT TO THREE-DIMENSIONAL PERIODIC GUSTS(U) NOTRE DAME UNIV IN AERODYNAMICS LAB H ATASSI 31 AUG 83 1983-12 AFOSR-TR-84-0757 1/1

UNCLASSIFIED AFOSR-82-0269 F/G 20/4 NL

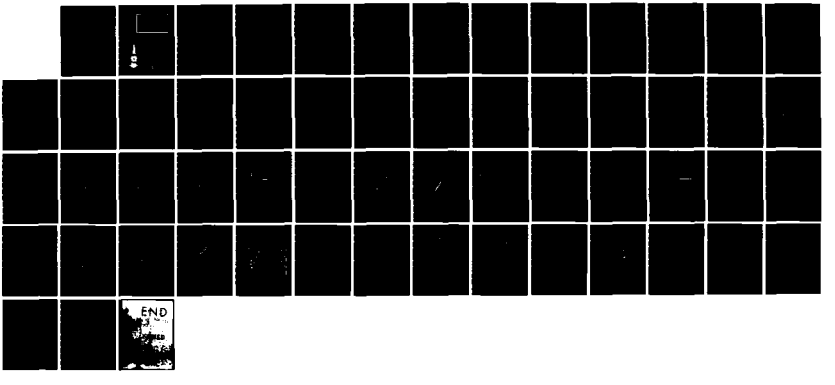

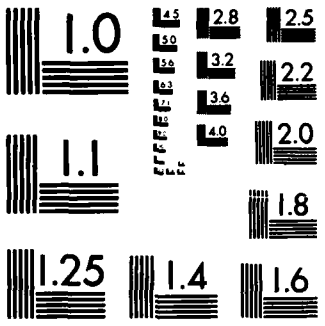

(4)

FINAL REPORT

TO THE

AIR FORCE OFFICE OF SCIENTIFIC RESEARCH

ON CONTRACT NO. 82-0269 ENTITLED

AERODYNAMICS OF AIRFOILS SUBJECT TO THREE-DIMENSIONAL PERIODIC GUSTS

Aerodynamics Laboratory

Department of Aerospace and Mechanical Engineering

University of Notre Dame

Notre Dame, Indiana 46556

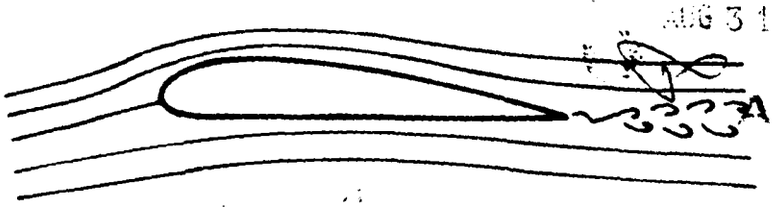

1983-12

UNCLASSIFIED
SECURITY CLASSIFICATION OF THIS PAGE

AD-A145149

REPORT DOCUMENTATION PAGE

1a. REPORT SECURITY CLASSIFICATION: UNCLASSIFIED	1b. RESTRICTIVE MARKINGS
2a. SECURITY CLASSIFICATION AUTHORITY	3. DISTRIBUTION/AVAILABILITY OF REPORT: Approved for Public Release; Distribution Unlimited.
2b. DECLASSIFICATION/DOWNGRADING SCHEDULE	
4. PERFORMING ORGANIZATION REPORT NUMBER(S)	5. MONITORING ORGANIZATION REPORT NUMBER(S): AFOSR-TR- 84 0757
6a. NAME OF PERFORMING ORGANIZATION: UNIVERSITY OF NOTRE DAME; 6b. OFFICE SYMBOL (If applicable)	7a. NAME OF MONITORING ORGANIZATION: AFOSR/NA
6c. ADDRESS (City, State and ZIP Code): DEPARTMENT OF AEROSPACE & MECHANICAL ENGR NOTRE DAME, IN 46556	7b. ADDRESS (City, State and ZIP Code): Bolling AFB, D.C. 20332
8a. NAME OF FUNDING/SPONSORING ORGANIZATION AIR FORCE OFFICE OF SCIENTIFIC RESEARCH; 8b. OFFICE SYMBOL (If applicable) AFOSR/NA	9. PROCUREMENT INSTRUMENT IDENTIFICATION NUMBER: AFOSR-82-0269
8c. ADDRESS (City, State and ZIP Code): BOLLING AFB, DC 20332	10. SOURCE OF FUNDING NOS.

PROGRAM ELEMENT NO.	PROJECT NO.	TASK NO.	WORK UNIT NO.
61102F	2307	A4	

11. TITLE (Include Security Classification) AERODYNAMICS OF AIR-FOILS SUBJECT TO THREE-DIMENSIONAL PERIODIC GUSTS (UNCLASSIFIED)

12. PERSONAL AUTHOR(S): H ATASSI

13a. TYPE OF REPORT	13b. TIME COVERED	14. DATE OF REPORT (Yr., Mo., Day)	15. PAGE COUNT
FINAL	FROM 1 Aug 82 TO 31 Aug 83	83, August 31	54

16. SUPPLEMENTARY NOTATION

17. COSATI CODES			18. SUBJECT TERMS (Continue on reverse if necessary and identify by block number)
FIELD	GROUP	SUB. GR.	UNSTEADY AERODYNAMICS PERIODIC GUSTS LIFTING AIRFOILS

19. ABSTRACT (Continue on reverse if necessary and identify by block number)

A general analysis of periodic three-dimensional vortical disturbances of streaming motions around streamlined and bluff bodies is developed using a unified approach wherein the mathematical problem is reduced to solving a single inhomogeneous wave equation with non-constant coefficients. In the limit of vanishing Mach number, the problem is formulated in terms of an inhomogeneous Fredholm integral equation of the second kind. The analysis is first applied to study the unsteady aerodynamics of an airfoil of arbitrary shape moving at low Mach number in a three-dimensional periodic gust pattern. Because the homogeneous equation has a non-trivial solution, a special procedure was developed for its solution and uniqueness is obtained by application of the Kutta condition at the trailing edge. The results were compared with those obtained from a nonlinear two-dimensional gust theory and linear oblique gust analyses. The comparison shows a very strong influence of the airfoil geometry and mean flow angle of attack and of the gust parameters on the unsteady lift and moment coefficients. In fact, depending on the

20. DISTRIBUTION/AVAILABILITY OF ABSTRACT	21. ABSTRACT SECURITY CLASSIFICATION
UNCLASSIFIED/UNLIMITED ☒ SAME AS RPT. ☐ DTIC USERS ☐	UNCLASSIFIED

22a. NAME OF RESPONSIBLE INDIVIDUAL	22b. TELEPHONE NUMBER (Include Area Code)	22c. OFFICE SYMBOL
Dr James D Wilson	202/767-4935	AFOSR/NA

DD FORM 1473, 83 APR EDITION OF 1 JAN 73 IS OBSOLETE.

84 08 30 031

UNCLASSIFIED
SECURITY CLASSIFICATION OF THIS PAGE

conditions considered, the unsteady lift and moment coefficients can be several times larger or smaller than those obtained from linear theories. A superposition principal was derived whereby the unsteady lift and moment acting on a thin airfoil with small camber and small angle of attack and subject to a two-dimensional gust can be constructed by linear superposition to the Sears lift and moment of three independent components accounting separately for the effects of airfoil thickness, airfoil camber and non-zero angle of attack of the mean flow. This is true in spite of the nonlinear dependence of the unsteady flow on the mean potential flow of the airfoil. Finally, the general analysis was applied to a streaming motion round a typical two-dimensional bluff body with harmonic vortical disturbances imposed upstream. For two-dimensional disturbances the unsteady velocity field is derived in terms of a double integral. The unsteady velocity and pressure fields are calculated to assess their variation particularly near the stagnation point.

FINAL REPORT

TO THE

AIR FORCE OFFICE OF SCIENTIFIC RESEARCH

ON CONTRACT NO. 82-0269 ENTITLED

AERODYNAMICS OF AIRFOILS SUBJECT TO THREE-DIMENSIONAL PERIODIC GUSTS

FOR THE PERIOD OF AUGUST 1, 1982 TO AUGUST 31, 1983

BY

H. ATASSI

PROFESSOR

DEPARTMENT OF AEROSPACE AND MECHANICAL ENGINEERING

UNIVERSITY OF NOTRE DAME

1983-12

TABLE OF CONTENTS

	ABSTRACT	iii
I.	INTRODUCTION	1
II.	AIRFOILS SUBJECT TO THREE-DIMENSIONAL PERIODIC GUSTS	3
III.	AIRFOIL IN A TWO-DIMENSIONAL PERIODIC GUST - NEW RESULTS	10
IV.	FLOW PAST A BLUFF BODY	12
V.	CONCLUSIONS	13
VI.	FUTURE PLANS	14
VII.	REFERENCES	16
	FIGURES	17
VIII.	PUBLICATIONS RESULTING FROM OUR WORK UNDER AFOSR SPONSORSHIP	49
XI.	PERSONNEL	49

A-1

ABSTRACT

A general analysis of periodic three-dimensional vortical disturbances of streaming motions round streamlined and bluff bodies is developed using a unified approach wherein the mathematical problem is reduced to solving a single inhomogeneous wave equation with non-constant coefficients. In the limit of vanishing Mach number, the problem is formulated in terms of an inhomogeneous Fredholm integral equation of the second kind.

The analysis is first applied to study the unsteady aerodynamics of an airfoil of arbitrary shape moving at low Mach number in a three-dimensional periodic gust pattern. Because the homogeneous equation has a non trivial solution, a special procedure was developed for its solution and uniqueness is obtained by application of the Kutta condition at the trailing edge. The results were compared with those obtained from a nonlinear two-dimensional gust theory and linear oblique gust analyses. The comparison shows a very strong influence of the airfoil geometry and mean flow angle of attack and of the gust parameters on the unsteady lift and moment coefficients. In fact, depending on the conditions considered, the unsteady lift and moment coefficients can be several times larger or smaller than those obtained from linear theories.

A superposition principle was derived whereby the unsteady lift and moment acting on a thin airfoil with small camber and small angle of attack and subject to a two-dimensional gust can be constructed by linear superposition to the Sears lift and moment of three independent components accounting separately for the effects of airfoil thickness, airfoil camber and non-zero angle of attack of the mean flow. This is true in spite of the nonlinear dependence of the unsteady flow on the mean potential flow of the airfoil.

Finally, the general analysis was applied to a streaming motion round a typical two-dimensional bluff body with harmonic vortical disturbances imposed upstream. For two-dimensional disturbances the unsteady velocity field is derived in terms of a double integral. The unsteady velocity and pressure fields are calculated to assess their variation particularly near the stagnation point.

I. INTRODUCTION - GENERAL OUTLINE OF OUR RESEARCH ACTIVITIES

The present research is a continuation of our previous work on the unsteady aerodynamics of lifting airfoils and turbomachine blades subject to three-dimensional vorticity disturbance (gusts) imposed upstream. The engineering relevance of this research derives from its direct application to the analysis of aeroelastic stability of aircraft structures such as wings, turbomachine engine components such as blades and guide vanes, helicopter rotor blades and newly-designed multi-blade propellers. Indeed all of these structural components are subject to fluctuating aerodynamic forces resulting from flow nonuniformities, which cause forced vibrations, eventually flutter and always generates unwanted noise.

The main objective of our research is to develop an aerodynamic theory and computational procedures to calculate the unsteady forces acting upon airfoils of arbitrary shape subject to three-dimensional gust disturbances. However the mathematical formulation which has evolved from our analytical work can also be applied under certain conditions to study the changes in turbulence and heat transfer characteristics of flows over bluff bodies. Therefore in addition to working on three-dimensional gusts interacting with airfoils, we have also carried out an analysis for periodic vortical disturbances acting upon a bluff body.

For small Mach numbers, the problem for a 3D gust is formulated in terms of an inhomogeneous Fredholm integral equation of the second kind around the airfoil contour. Since the homogeneous equation has a non-trivial solution, a special numerical procedure has been devised for its solution. The uniqueness is obtained by application of the Kutta condition at the trailing edge. The unsteady lifts and moments acting on Joukowski's airfoils of various geometry and incidence and subject to different upstream gust conditions were

calculated. The results were first compared to our work on two-dimensional gusts acting on thin lifting airfoils where we have derived analytical expressions for the lift function. Excellent agreement was obtained for conditions within the validity of the derived analytical formulas. The results were also compared with those obtained from linear oblique gust analyses. The comparison indicates a very strong influence of the airfoil geometry and mean flow angle of attack on the unsteady lifts and moments. These effects are due to the nonlinear dependence of the vorticity disturbances on the mean flow as they propagate downstream and interact with the airfoil. In fact, depending on the conditions considered, the unsteady lifts and moments of a lifting airfoil can be several times smaller or larger than those obtained from linear theories. <u>These results can lead to a significant reduction of forced vibration of structural components if they are incorporated in turbomachine stage and blade design</u>.

A spin-off of revisiting our two-dimensional theory of a two-dimensional gust acting on thin lifting airfoils is that we were able to derive the following new and important result.

> For a thin airfoil with small camber and small angle of attack moving in a periodic gust pattern, the unsteady lift and moment caused by the gust can be constructed by linear superposition to the Sears lift and moment of three independent components accounting separately for the effects of airfoil thickness, airfoil camber and non-zero angle of attack of the mean flow.

This result is true in spite of the <u>nonlinear dependence</u> of the unsteady flow on the mean potential flow of the airfoil. This brings about a considerable simplification of the derivation of the unsteady lift formula as well as of

its practical applications.

Finally, we have also applied the general theory to a streaming motion around a typical two-dimensional bluff body with harmonic vortical disturbances imposed upstream. The expression for the velocity field is derived in terms of a double integral and there is no need to solve an integral equation for two-dimensional disturbances. The unsteady velocity and pressure fields are calculated in the neighborhood of the stagnation point where the strongest effects on the flow disturbance occurs. This yields the transfer function that relates the local and upstream velocity fields. Thus, within the approximation of the rapid distortion theory of turbulence, the velocity correlations of the local turbulent flow can be calculated from the spectrum of the velocity correltions of the upstream turbulence.

II. AIRFOILS SUBJECT TO THREE-DIMENSIONAL PERIODIC GUST

A schematic of an airfoil moving in a periodic gust pattern is shown in Figure 1. Since the gust velocity is small compared to the mean velocity U of the flow, we can, without loss of generality consider for the purpose of the analysis a harmonic component of the form

$$\vec{u}_\infty = \vec{a} \exp\{i(\vec{k}\cdot\vec{x} - k_1 t)\} , \tag{1}$$

where

$$\vec{a} = a_1\vec{i}_1 + a_2\vec{i}_2 + a_3\vec{i}_3 , \tag{2}$$

and

$$\vec{k} = k_1\vec{i}_1 + k_2\vec{i}_2 + k_3\vec{i}_3 . \tag{3}$$

$(\vec{i}_1, \vec{i}_2, \vec{i}_3)$ are unit vectors forming a positive triad. $\vec{i}_1$ is in the direction of the upstream mean velocity $\vec{U}$ and $\vec{i}_3$ is in the span direction. All

velocities and lengths are nondimensionalized with respect to U and c/2, respectively, c being the airfoil chord length; and the time t is normalized with respect to c/2U. Thus k_1 is the usual reduced frequency. $\vec{k}$ represents the direction of propagation of the gust. Note that the continuity equation requires

$$\vec{a} \cdot \vec{k} = 0 \tag{4}$$

It is significant to note that for a two-dimensional gust, condition (4) defines the longitudinal (a_1) and trannsverse (a_2) gust components in terms of the wave numbers k_1 and k_2, and the magnitude of the gust disturbance $|\vec{a}|$. Therefore it is customary to normalize the gust with respect to $|\vec{a}|$ and consider the two independent parameters k_1 and k_2. For a three-dimensional gust there are six parameters defining the upstream conditions of the gust ($\vec{a}$ and $\vec{k}$). Using condition (4) and normalizing the gust with respect to $|\vec{a}|$ still leaves us with <u>four</u> independent parameters. We choose as independent parameters the three wave numbers k_1, k_2 and k_3 and the angle of the projected initial disturbance in the plane perpendicular to the span direction (the ratio a_2/a_1). Indeed, the wave numbers enter the governing equation and determine its character. In addition, they are determined from the machine design. The parameters (a_1, a_2, a_3) do not determine the character of the governing equation and are usually data to be input in the calculations from secondary flow measurement.

Further details on the theory are given in [1,2,3]. Here we present only the most significant results.

The unsteady forces and moments will be nondimensionalized as follows by introducing the lift coefficient

$$C_{L'} = \frac{L'}{\pi\rho cU|\vec{a}|\ \exp(-ik_1 t)} \quad , \tag{5}$$

The drag coefficient

$$C_{D'} = \frac{D'}{\pi\rho cU|\vec{a}|\ \exp(-ik_1 t)} \quad . \tag{6}$$

and the moment coefficient

$$C_{M'} = \frac{M'}{\frac{1}{2}\pi\rho c^2 U|\vec{a}|\ \exp(-ik_1 t)} \tag{7}$$

where L', D' and M' denote lift, drag and moment unit per span, respectively.

In all the following results the phase of the gust will be referenced with respect to the middle point of the airfoil defined as the middle point on the airfoil camber line. This is equivalent to using the system of coordinates $(x_2\text{-}y_2)$ for the airfoil cross section shown in Figure 2, the x_2-axis being in the direction of the mean flow far upstream. This convention will enable us to compare our results directly with those of the linear theories of von Karman and Sears [4], Sears [5] and Graham [6], where the gust is referenced with respect to the flat plate midpoint. Our convention will also coincide with that adapted by Goldstein and Atassi [7] and Atassi [8] for thin airfoils in a two-dimensional gust and thus our results will also compare with [7] and [8].

To check the validity of our computation scheme two sets of comparisons were carried out. First we considered a two-dimensional gust with transverse and longitudinal components. We also chose airfoils with small camber, small thickness and small angle of attack to the mean flow so that our results will compare with the fully analytical results in [7] and [8]. Figure 3 is a vector diagram showing the real and imaginary parts of the unsteady lift

coefficient versus the reduced frequency k_1 for an airfoil with a thickness ratio of 0.05 at 5° incidence to the mean flow. The gust is propagating at 45° ($k_1=k_2$). The present results are denoted by PRT and the results obtained from [7] and [8] are denoted by SOT (second order theory). Excellent agreement is obtained for a reduced frequency range of 0.25 to 2.5. The slight difference is due to the fact that the analytical results were for zero-thickness airfoils. Figure 4 shows similar results for an airfoil at zero angle of attack to the mean flow but with 0.05 camber and 0.05 thickness ratio. Again excellent agreement is obtained between present results and SOT. However, as we increase the parameters characterizing the mean flow, that is as the distortion of the gust is increased, a large discrepancy between our present results and SOT appears. Figure 5 shows this comparison for an airfoil with 0.05 camber and 0.05 thickness ratio, placed at 5° angle of attack to the mean flow. As expected, the difference between PRT and SOT becomes larger as the reduced frequency is increased. This is due to the fact that SOT is valid only in the limit $\alpha k_1 << 1$, where α is a parameter characterizing the mean flow departure from the uniform state. Thus for the same α, as k_1 is increased, second order nonlinear effects become more significant. Figure 6 remarkably shows how the nonlinear effects for a highly cambered airfoil (15% camber) become particularly pronounced at reduced frequencies larger than unity. Note that for the airfoils shown in Figures 5 and 6, the value of the parameter α is about 0.25 and 0.35, respectively. Thus one should not expect SOT to be valid at large k_1.

The other set of comparisons we have carried out was with Graham's results [6] for a flat plate in an oblique gust ($k_3 \neq 0$). Figure 7 shows plots of the unsteady lift coefficient obtained from our results (PRT) for an airfoil of thickness ratio 0.05 and those of Graham for a frequency

range of 0.1 to 2.5. It is seen that very good agreement is obtained for this frequency range even though at higher frequency the effects of thickness become more important.

We now turn to assess the importance of the parameters of the three-dimensional gust and the airfoil mean flow. We first considered a thin airfoil (0.05 thickness) with small camber (0.05 camber) as shown in Figure 8. The airfoil is placed at 5° angle of attack to the mean flow. The upstream gust conditions were $a_3 = 0$ and $k_2 = k_1$. That is the initial disturbance was in a plane perpendicular to the airfoil span and at 45° to the upstream mean flow. The gust will propagate obliquely with k_3 as a parameter. Figures 9, 10 and 11 show vector diagrams of the real and imaginary parts of the unsteady lift coefficient, the unsteady moment coefficient and the unsteady drag coefficient, respectively, the reduced frequency k_1 being varied from 0.25 to 2.5 for values of the parameter k_3 equal to 0.25, 0.5, 1.0 and 2.0. Examination of Figure 9 shows that the spanwise wavenumber, k_3 or in other words the obliqueness of the gust, has a very strong influence on the unsteady lift coefficient. As k_3 is increased the magnitude of the unsteady lift is significantly reduced. For example at $k_1 = 0.5$, the magnitudes of the unsteady lift coefficients are 2.1, 1.1 and 0.5 for $k_3 = 0.25$, 1.0 and 2, respectively. The effects of k_3 on the unsteady moment coefficient are still very significant at low reduced frequency but as shown in Figure 10 they are not as pronounced as for the unsteady lift coefficient for higher frequency. Finally, as we examine Figure 11 we see that the effect of k_3 on the unsteady drag coefficient is only significant at low reduced frequency and essentially nil at higher frequency.

The relatively simple choice of the gust parameters for the cases shown in Figures 9, 10 and 11 affords a comparison with the linear oblique gust case

of Figure 7 and that of SOT in Figure 5. Indeed, the upstream gust conditions for Figures 7 and 9 can be considered to be the same since taking $k_2 = k_1$ and $a_1 = -a_2$ instead of zero for both would only reduce the magnitude of the gust by a factor of $1/\sqrt{2} \sim 0.71$. The unsteady lift coefficient is considerably reduced at low reduced frequency even with 5° angle of attack and 5% camber (thickness does not seem to have a significant influence). For example at $k_1 = 0.5$, Figure 9 gives $C_{L'} \sim 0.12$, while in the flat plate case it would be 0.21. Comparison between Figures 5 and 9 shows that the effect of k_3 on the unsteady lift becomes very significant as k_3 is increased to about unity.

We now consider an airfoil with high steady lift coefficient and whose potential flowfield exhibits significant variations from the uniform upstream conditions. Such an airfoil is shown in Figure 12. It has 10% camber and 10% thickness ratio and is placed at 10° angle of attack to the meanflow. Again the upstream gust conditions were $a_3 = 0$ and $k_2=k_3$. These conditions are similar to the case of the airfoil with small steady lift studied above. Figures 13 and 14 show the variation of the real and imaginary components of the unsteady velocity along the airfoil surface versus the arc length S of the airfoil counted from the stagnation point (S=0 corresponds to the airfoil stagnation point). The variation of the unsteady velocity component along the steady streamline are also plotted ahead of the stagnation point (S<0). The discontinuity seen at S=0 in the velocity is due to the fact that ahead of the stagnation point, the plotted velocity is indeed normal to the airfoil and thus is zero at $S = 0$. The unsteady velocity at the stagnation point is finite which indicates that the unsteady pressure at this location is also finite. Note the large variation of the velocity on the airfoil suction side because of the large airfoil curvature. The discontinuity at the trailing edge between the velocities at the suction and pressure sides represents the strength of the vortex sheet extending from the trailing edge in the airfoil

wake. The unsteady pressure distribution is shown in Figure 15.

Figure 16 shows a vector diagram showing the real and imaginary part of the unsteady lift coefficient versus the reduced frequency. Graham's results for an oblique gust acting on a flat plate airfoil are also plotted for comparison. It is clearly seen that the magnitude and phase are totally different for the two cases at all reduced frequencies. The significant reduction of the magnitude of the lift is not necessarily valid for different gust conditions. Figure 17 shows the real and imaginary components of the unsteady lift but now compared with our second order theory (SOT). Again, the influence of the obliqueness of the gust through the spanwise wavenumber k_3 is very significant. Figure 18 shows plots of the unsteady lift coefficients for different values of k_3. Note that k_3 influences the unsteady lift coefficients at all reduced frequencies while for an airfoil with small loading k_3 seems to have stronger influence at low frequencies.

Figure 19 shows the unsteady moment coefficient with Graham results plotted for comparison. The results seem to be quite different from those of the linear theory and even from those of the airfoil with small loading shown in Figure 10. The effects of the gust obliqueness on the unsteady moment are shown in Figure 20. As for the case of the airfoil with small loading (see Figure 19) the influence of k_3 is larger at low reduced frequency. However, even at large reduced frequency the influence of k_3 is still significant. The unsteady drag coefficients are shown in Figure 21 and indicate a much stronger k_3 influence with increased airfoil loading.

Finally we considered the general case of a gust with upstream disturbances having a non-zero spanwise component ($a_3 \neq 0$). Because the gust depends on four independent parameters, we imposed the conditions $k_2 = k_1$ and $a_2/a_1 = -7/4$ with $a_2 > 0$. Figure 22 shows the variation of the unsteady lift

coefficient caused by this gust on the same airfoil and mean flow angle of attack as in Figure 12. It is significant to compare these results with those of Figure 18. They are clearly very different and unrelated. This underlines the complexity of the present problem.

III. AIRFOIL IN A TWO-DIMENSIONAL PERIODIC GUST - NEW RESULTS

For a two-dimensional periodicity gust ($a_3 = 0$) interacting with an airfoil a second order theory was developed in [7]. The theory accounts for the dependence of the unsteady flow on the mean potential flow of the airfoil. However, in order to obtain a relatively simple closed-form solution, the analysis was restricted to the case of a thin airfoil with small angle of attack and small camber. A general formula was then derived for the unsteady lift caused by the gust,

$$L' = L'_o + \alpha L'_1 \quad , \tag{8}$$

where

$$L'_o = \pi\rho cU|\vec{a}| \frac{k_1}{|\vec{k}|} \exp(-ik_1 t)\, \bar{S}(k_1) \tag{9}$$

is the fluctuating lift derived by Sears [5] for a flat plate at zero-incidence and where $S(k_1)$ is the Sears function. α is a small parameter which characterizes the mean flow disturbance and L'_1 is a function of k_1, k_2, and the parameters β, m and θ, where $\alpha\beta$ is the angle of attack, αm is the airfoil camber and $\alpha\theta$ is the airfoil thickness ratio. Examination of the expression for L'_1 derived in [7] will lead to the conclusion that there is a nonlinear dependence of L'_1 on the steady-state aerodynamics, i.e., it is not possible to superpose the effects of thickness, camber and angle of attack to the mean flow.

However, re-examination of the theory led us to derive the following remarkable result:

> for a thin airfoil with small camber and angle of attack moving in a periodic gust pattern, the unsteady lift L_1' can be constructed by linear superposition of three independent components: $L_{1\beta}'$ resulting from a non-zero angle of attack of the mean flow, L_{1m}' resulting from the airfoil camber and $L_{1\theta}'$ produced by its thickness.

Therefore the unsteady lift L_1' can be written as

$$L_1'(k_1,k_2,\beta,m,\theta) = \beta L_{1\beta}'(k_1k_2) + mL_{1m}'(k_1,k_2) + \theta L_{1\theta}'(k_1,k_2) \qquad (10)$$

The expressions for $L_{1\beta}'$, L_{1m}' were then derived and analyzed to assess the effect of airfoil camber and mean flow angle of attack, Figures 23, 24, 25 and 26 show the variation of the real and imaginary parts of

$$R_\beta = \frac{L_{1\beta}'}{\pi\rho cU|\vec{a}|\exp(-ik_1t)}, \qquad (11)$$

and

$$R_m = \frac{L_{1m}'}{\pi\rho cU|\vec{a}|\exp(-ik_1t)}, \qquad (12)$$

versus the reduced frequency k_1 for different values of the transverse wavenumber k_2. Details are given in [8].

IV. FLOW PAST A BLUFF BODY

As an illustration of the general theory we have also studied a streaming motion around a typical two-dimensional bluff body with upstream imposed harmonic vortical disturbance. Hunt [9] studied the flow past a circular cylinder but his solution could not give the detailed behavior near the stagnation point for arbitrary reduced frequency. Here we consider a typical bluff body as shown in Figure 27. For such a body the potential flow approximation of the mean flow is more realistic than for the circular cylinder used by Hunt where the potential flow is only valid in the frontal part of the body.

The potential flow is obtained by superposing a uniform flow to a source at the origin. Once the potential function is known it is easy to construct the Green's function satisfying Neumann's boundary conditions along the body. Therefore, the unsteady disturbance velocity can be cast simply as a double integral as shown in [1 and 2].

The unsteady velocity and pressure fields were calculated in the neighborhood of the stagnation point as shown in Figure 28. The points where these fields were calculated correspond to the intersection of the lines ϕ_0 = constant and ψ_0 = constant, where ϕ_0 and ψ_0 represent the potential and stream functions of the mean flow. Figures 29, 30 and 31 show three-dimensional diagrams of the variation of the magnitude of the unsteady tangential velocity, normal velocity and pressure versus ϕ_0 (FI) and ψ_0 (PSI). Figure 32 shows the variation of the magnitude of the pressure along the stagnation streamline $\psi_0 = 0$. Note that the velocities are finite at the stagnation point but exhibit large gradients. The pressure gradient is smooth ahead of the stagnation point but exhibit large variations along the body.

V. CONCLUSIONS

The analysis we have carried out for periodic three-dimensional vortical disturbances of streaming motions round streamlined and bluff bodies fully accounts for the nonlinear dependence of the unsteady flow on the mean potential flow of the body. Its application to the case of an airfoil of arbitrary shape moving in a three-dimensional periodic gust pattern is, to our best knowledge, the first treatment of the general gust problem.

The results we have obtained thus far enable us to point out certain important conclusions regarding the unsteady aerodynamic coefficients.

1. Use of linear flat plate theories to predict gust loading could lead to totally erroneous results even for moderately lifting airfoils.
2. The obliqueness of the gust always tends to reduce the magnitude of the gust response.
3. The influence of the gust initial conditions (for the same wave numbers k_1, k_2, k_3) is very strong as shown by comparison of Figures 18 and 22.
4. For the same airfoil, the aerodynamic coefficients can be several times larger or smaller than those obtained for a reference flat plate airfoil depending on the choice of the gust initial conditions represented by the wave numbers k_1, k_2 and k_3 and by the gust initial components represented by the parameters a_1, a_2 and a_3.

These results can lead to a significant reduction of forced vibration of structural components if they are incorporated in the machine design. However, in order to gain more insight on how to affect the gust parameters for reducing the unsteady aerodynamic coefficients, a parametric study of the

gust response is needed. This study should also be coupled with simulation of commonly observed configurations of nonuniform flows such as wakes, tip and hub vortices, and secondary flows. Indeed these nonuniform flow configurations directly affect the gust initial parameters.

VI. FUTURE PLANS

Our future plans are determined by the present state in unsteady aerodynamic modeling and technological needs. Let us briefly review the problems which we feel should be developed in response to ongoing technological developments.

1. Interaction of Wakes and Swirling Vortices with Loaded Airfoils

In turbomachines, major upstream disturbances of uniform flow are caused either by viscous wakes or by swirling vortices emanating from upstage tips. In order to reduce forced vibrations, it is important for the designer to know the parameters that strongly affect the unwanted fluctuating forces. This study is indeed a follow-up to the work presented here. A parametric study of the effects of the gust initial parameters coupled with wake and vortex simulation would determine an optimization procedure for reducing these unwanted forces. This should lead to interesting conclusions in view of the observed strong influence of the gust parameters on the unsteady aerodynamic coefficients.

2. Compressibility Effects

Most turbomachine blading systems operate at transonic velocities. The effects of a high Mach number are very significant for flat plate airfoils. Our general anaysis applies directly to the transonic airfoil case. The governing equation is though more difficult to solve. However, our present experience at low Mach numbers should provide a basis for comparison to more elaborate numerical schemes.

3. Cascade Effects

Depending on the solidity and stagger, cascade effects can be very important, as shown in our previous work on the oscillating cascade. An extension of the present analysis to the case of a cascade can be done without significant difficulty except for the added computational time due to determining the mean flow of the cascade.

4. Rotor and Propeller Problems

The mean flow past a rotor or a multi-blade propeller is rotational in a frame of reference fixed with respect to the rotor/propeller. This raises certain difficulty as to the formulation of the problem. We feel certain analytical work is needed to extend our present approach to this important class of problems.

VII. REFERENCES

1. Atassi, H., "Aerodynamics of Airfoils Subject to Three-Dimensional Periodic Gusts," University of Notre Dame Report 1982-10.

2. Atassi, H., "A Uniformly Valid Splitting of Unsteady Vortical and Entropic Disturbances of Potential Flows," to be submitted to the Journal of Fluid Mechanics.

3. Atassi, H., and Grzedzinski, J., "Three-Dimensional Periodic Vortical Disturbances Acting Upon an Airfoil," to be submitted to the Journal of Fluid Mechanics.

4. vonKarman, T., and Sears, W.R., "Airfoil Theory for Nonuniform Motion," Journal of Aeronautical Sciences, Vol. 5, No. 10, 1938, pp. 6-25.

5. Sears, W.R., "Some Aspects of Nonstationary Airfoil Theory and its Practical Applications," Journal of Aeronautical Sciences, Vol. 8, No. 3, 1941, pp. 104-198.

6. Graham, J.M.R., "Lifting Surface Theory for the Problem of an Arbitrary Yawed Sinusoidal Gust Incident on a Thin Airoil in Incompressible Flow," Aeronautical Quarterly, Vol. XXI, Part 2, May 1972, p. 182.

7. Goldstein, M.E., and Atassi, H., "A Complete Second Order Theory for the Unsteady Flow About an Airfoil Due to a Periodic Gust," Journal of Fluid Mechanics, Vol. 74, 1976, pp. 741-765.

8. Atassi, H., "The Sears Problem for a Lifting Airfoil Revisited - New Results," Journal of Fluid Mechanics, Vol. 141, 1984, pp. 102-122.

9. Hunt, J.C.R., "A Theory of Turbulent Flow Round Two-Dimensional Bluff Bodies," Journal of Fluid Mechanics, Vol. 61, 1973, pp. 625-706.

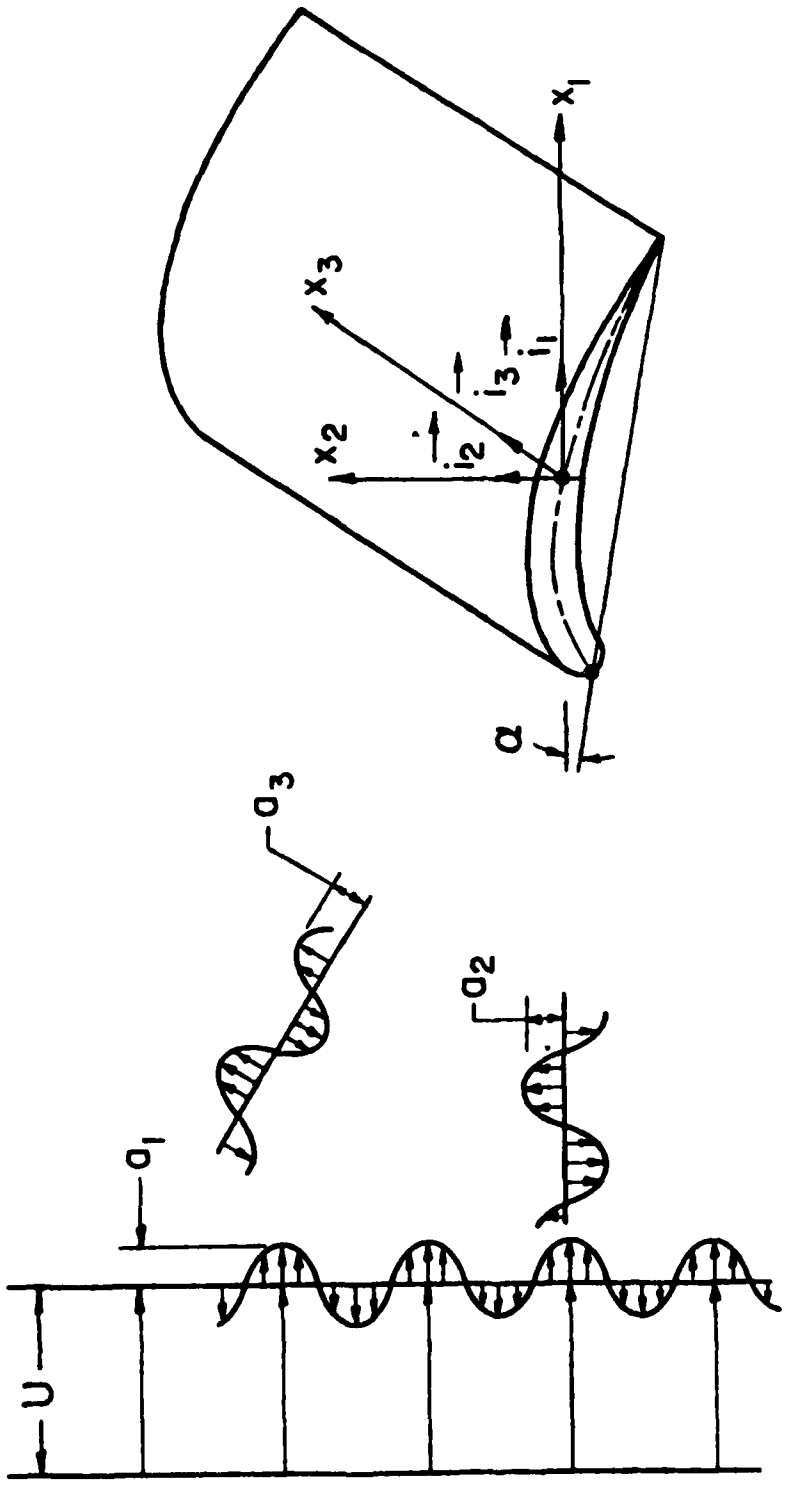

FIGURE 1. AIRFOIL IN A THREE-DIMENSIONAL GUST

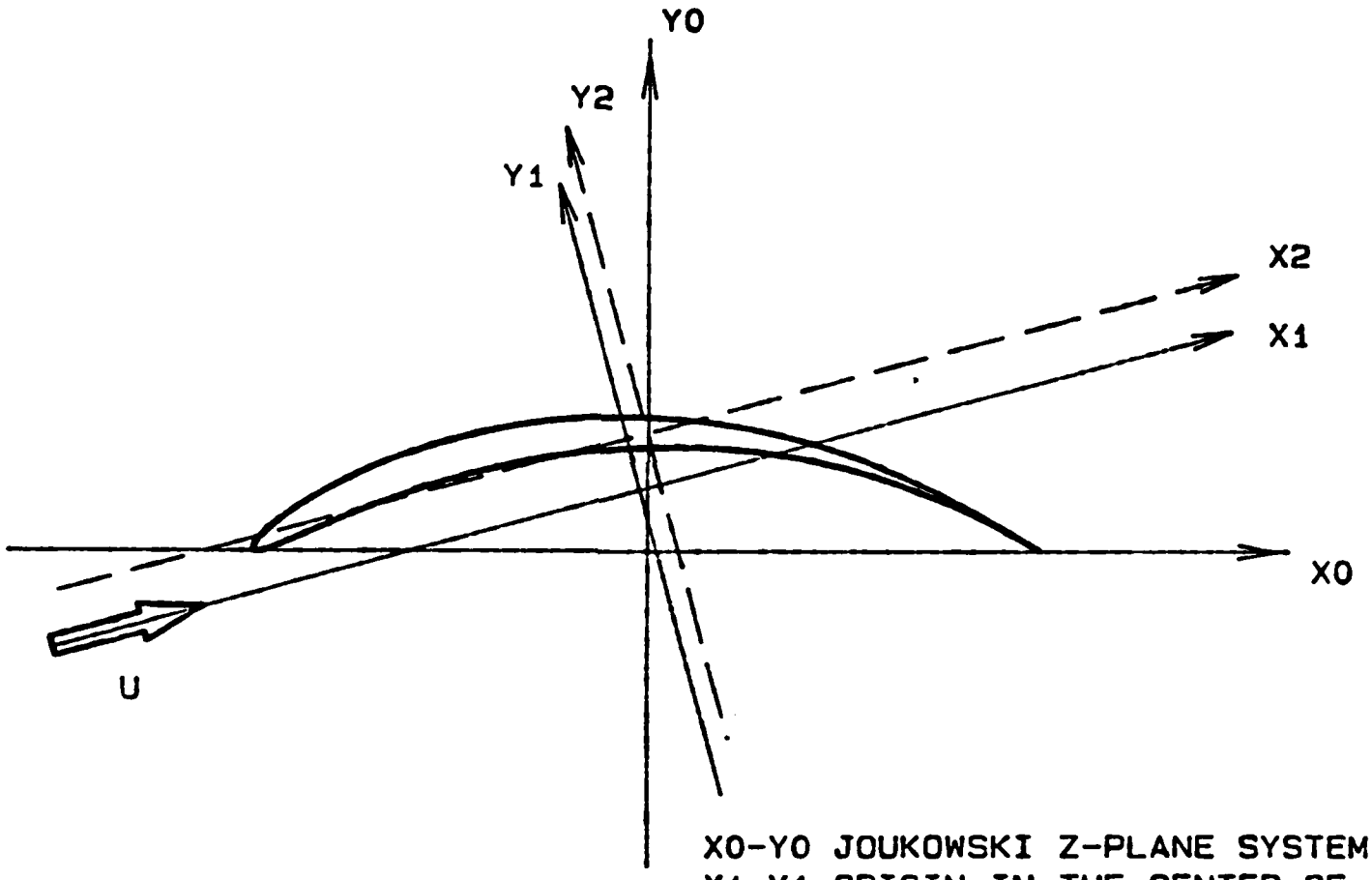

FIGURE 2. SYSTEMS OF COORDINATES

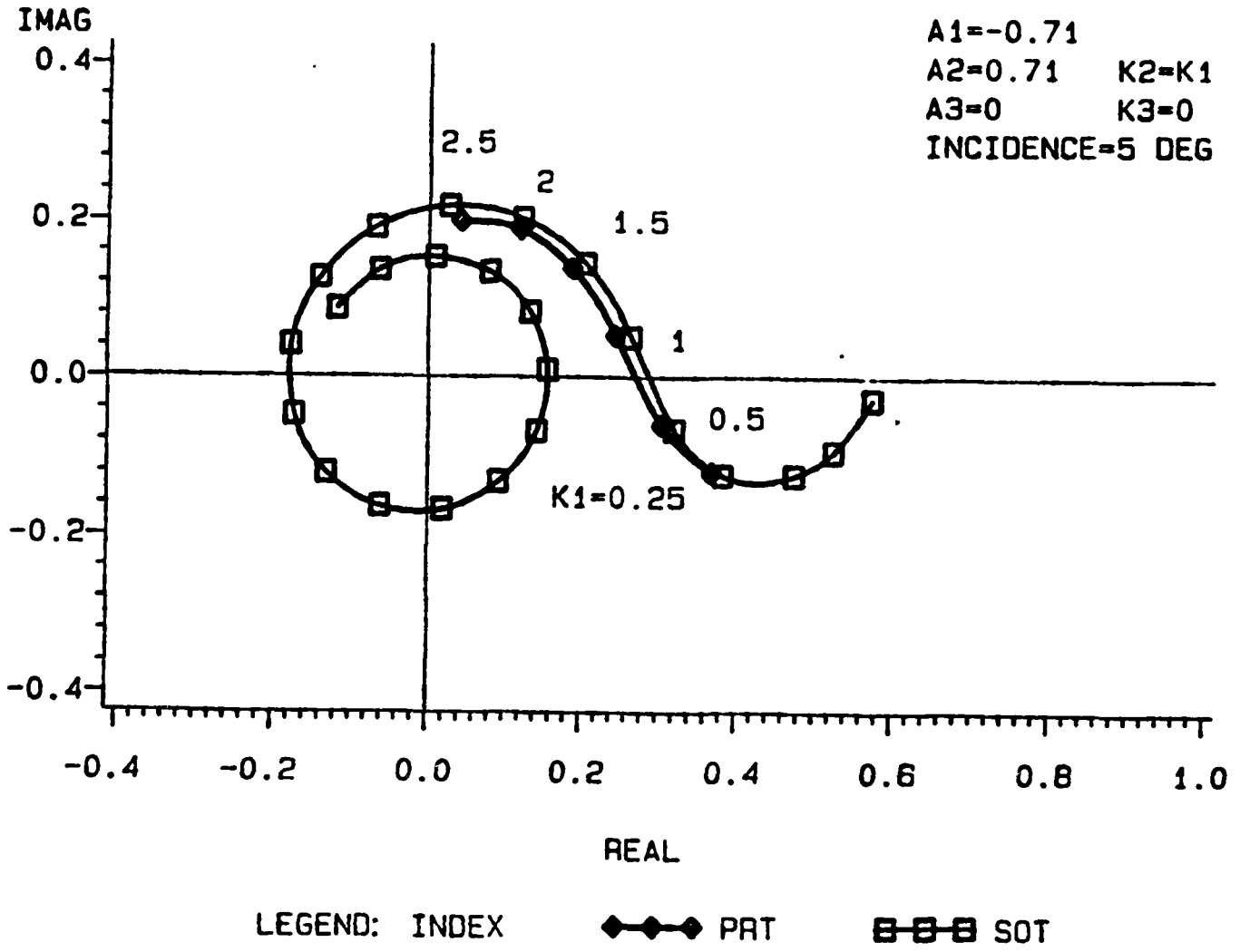

FIGURE 3. THE UNSTEADY LIFT COEFFICIENT
JOUKOWSKI AIRFOIL: CAMBER=0 THICKNESS=0.05

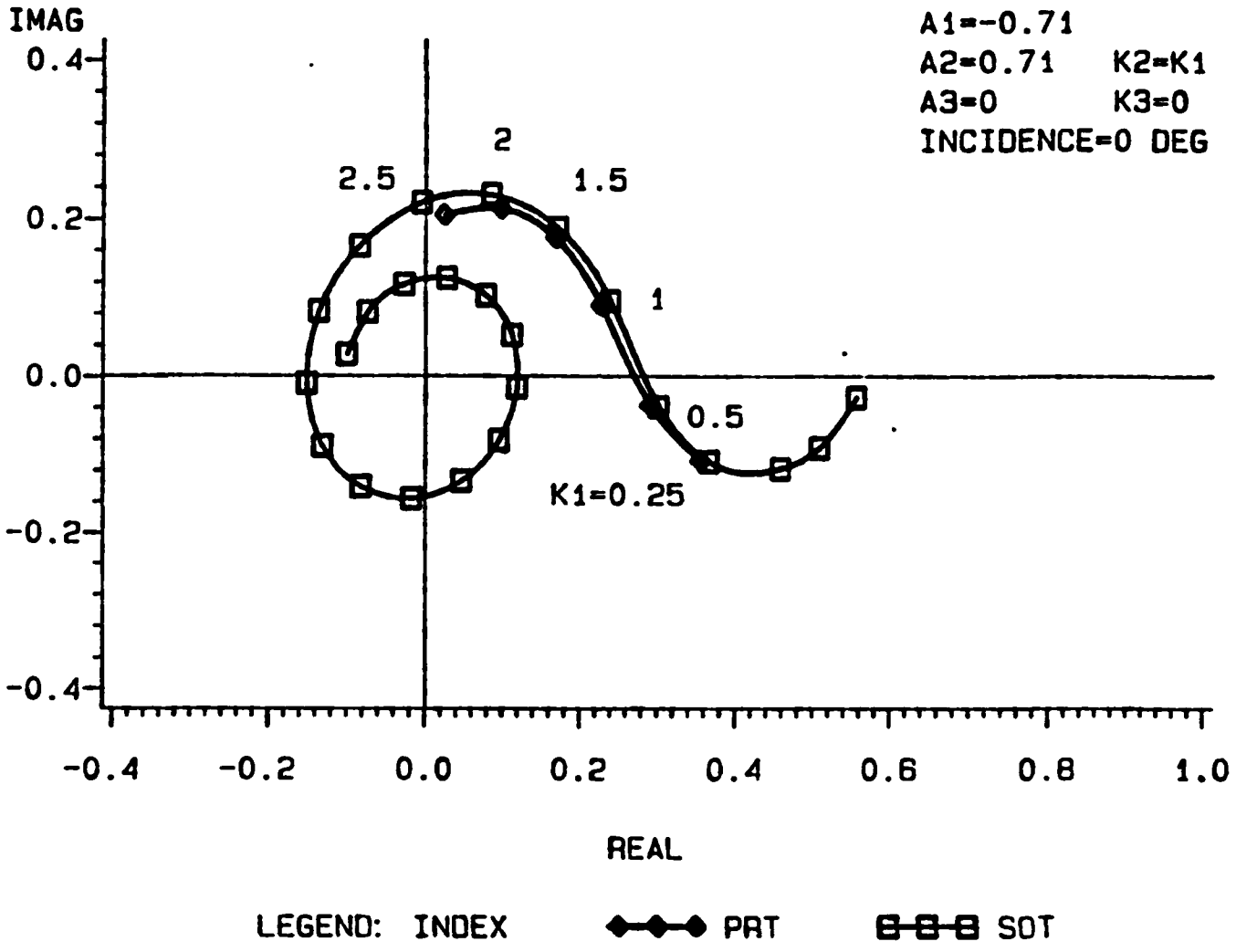

FIUGRE 4. THE UNSTEADY LIFT COEFFICIENT
JOUKOWSKI AIRFOIL: CAMBER=0.05 THICKNESS=0.05

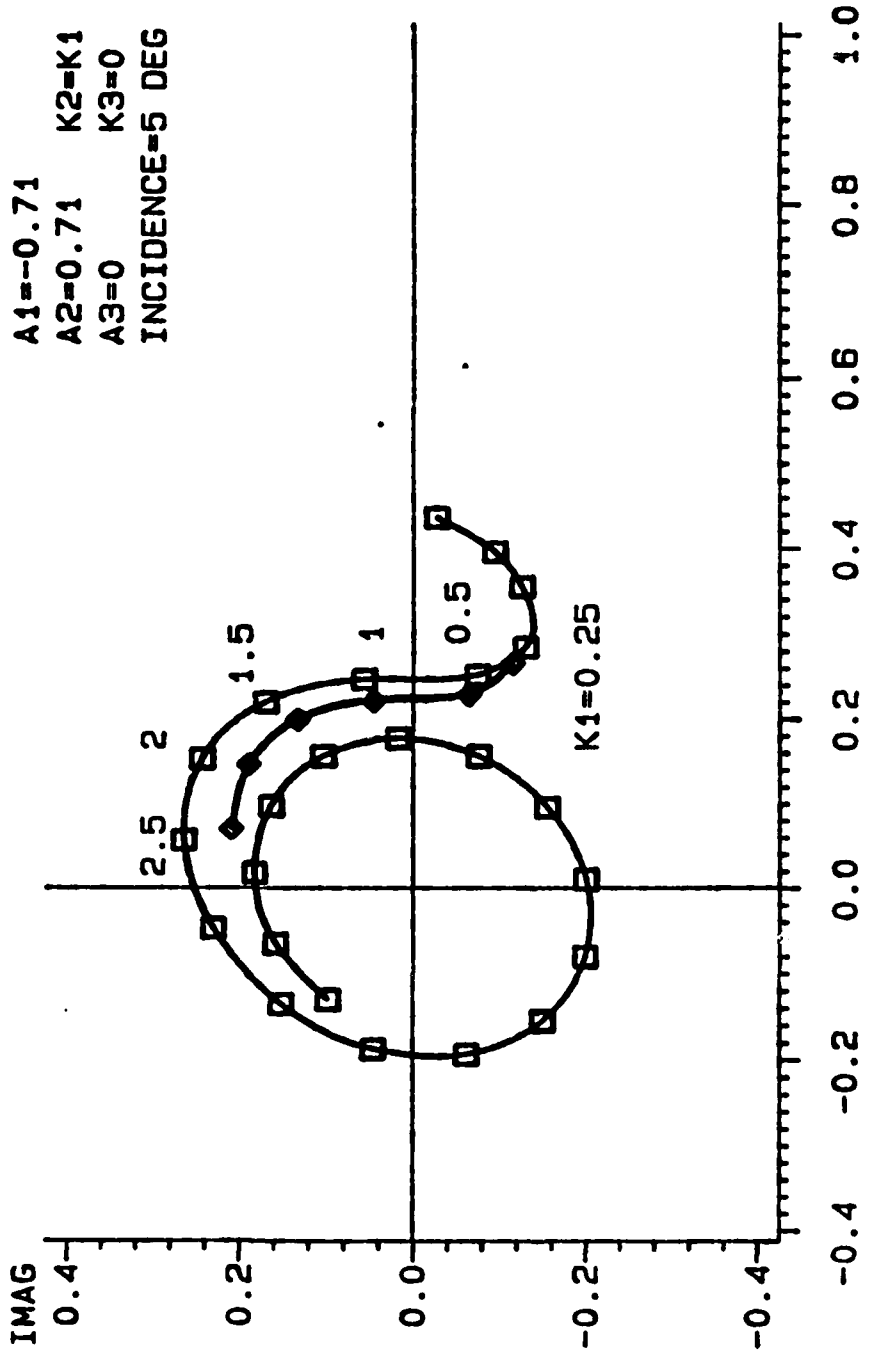

FIGURE 5. THE UNSTEADY LIFT COEFFICIENT
JOUKOWSKI AIRFOIL: CAMBER=0.05 THICKNESS=0.05

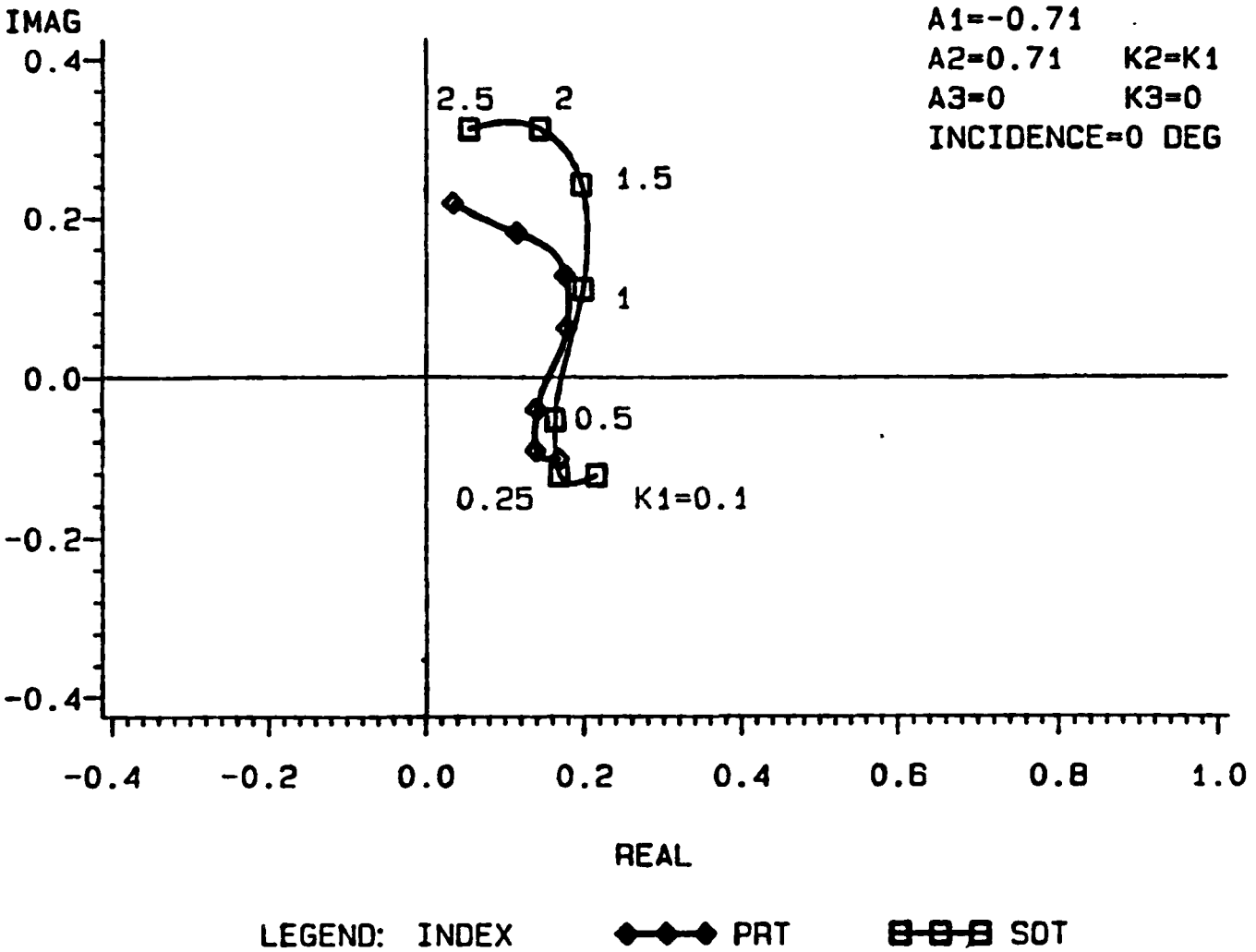

FIGURE 6. THE UNSTEADY LIFT COEFFICIENT
JOUKOWSKI AIRFOIL: CAMBER=0.15 THICKNESS=0.05

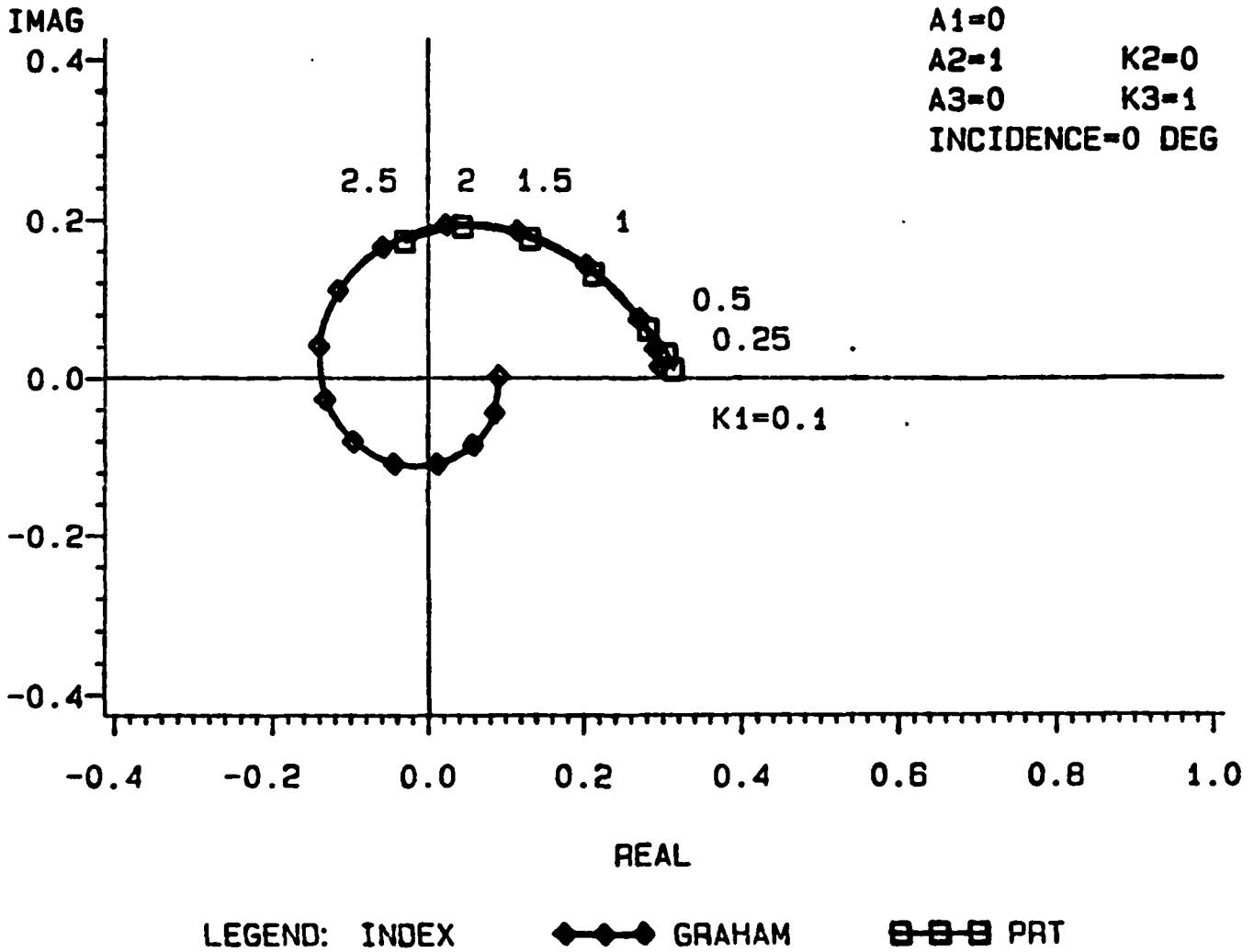

FIGURE 7. THE UNSTEADY LIFT COEFFICIENT
JOUKOWSKI AIRFOIL: CAMBER=0 THICKNESS=0.05

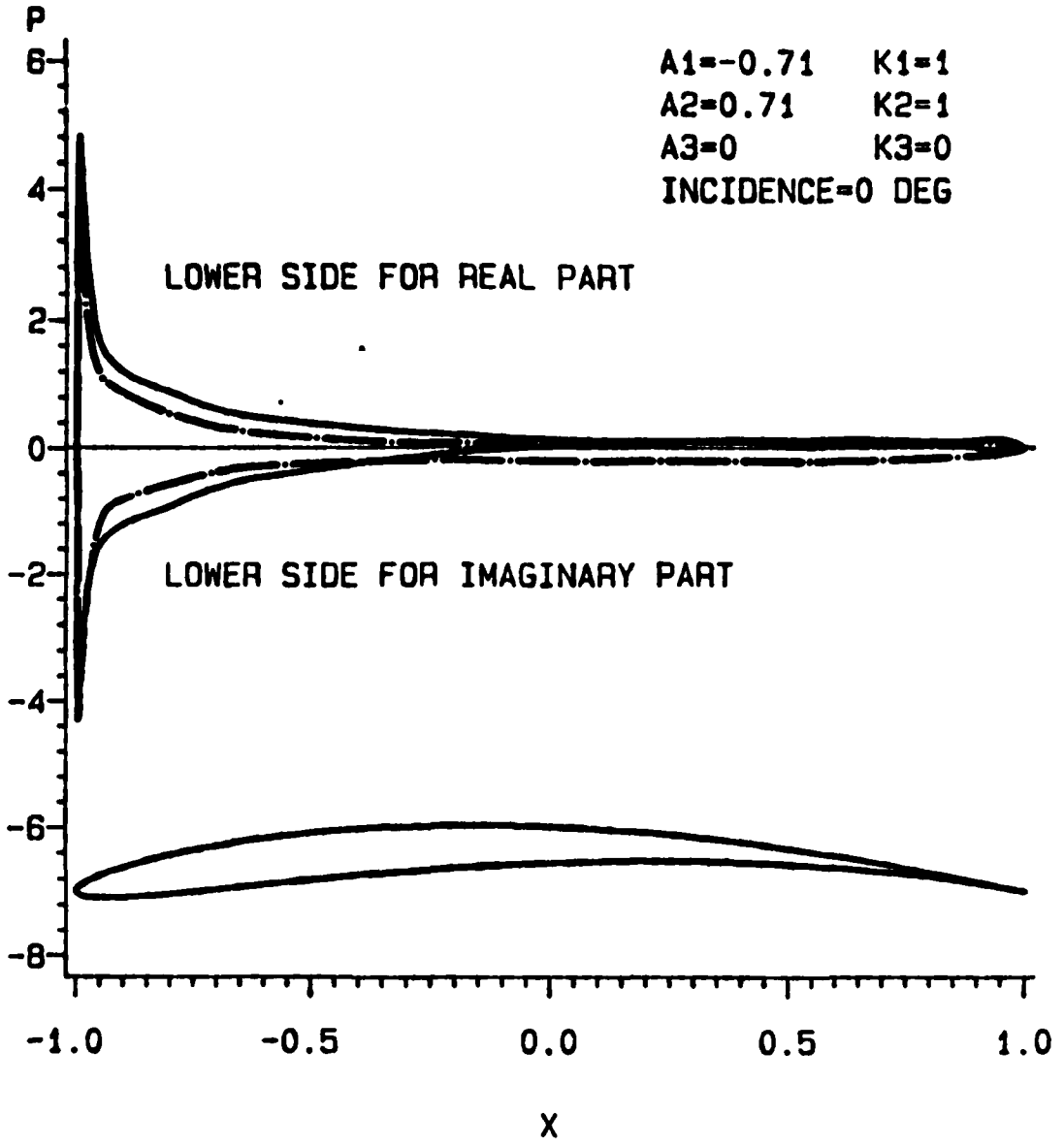

UNSTEADY PRESSURE

FIGURE 8. REAL (SOLID LINE) AND IMAGINARY (DASHED LINE)
JOUKOWSKI AIRFOIL: CAMBER=0.05 THICKNESS=0.05

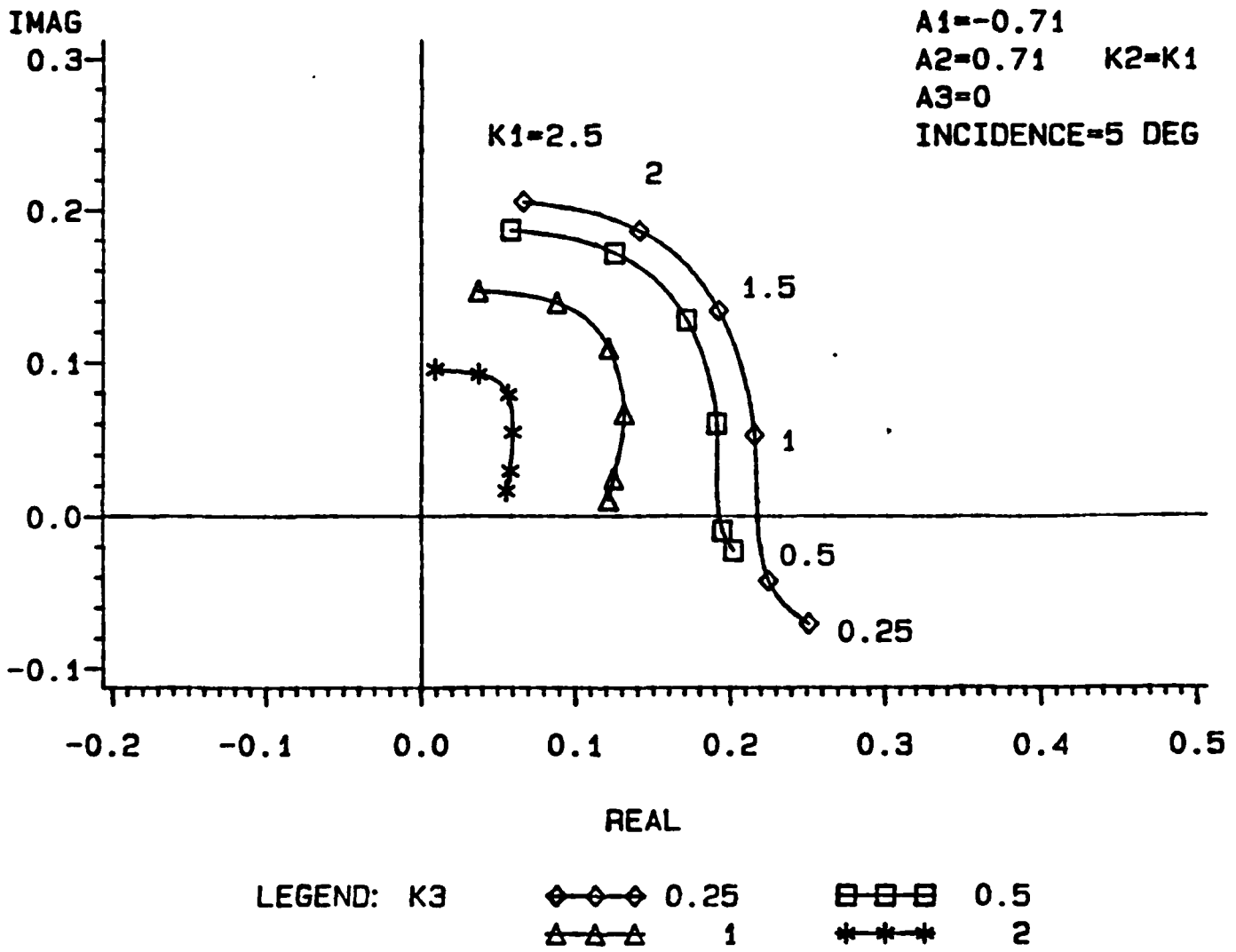

FIGURE 9. THE UNSTEADY LIFT COEFFICIENT
JOUKOWSKI AIRFOIL: CAMBER=0.05 THICKNESS=0.05

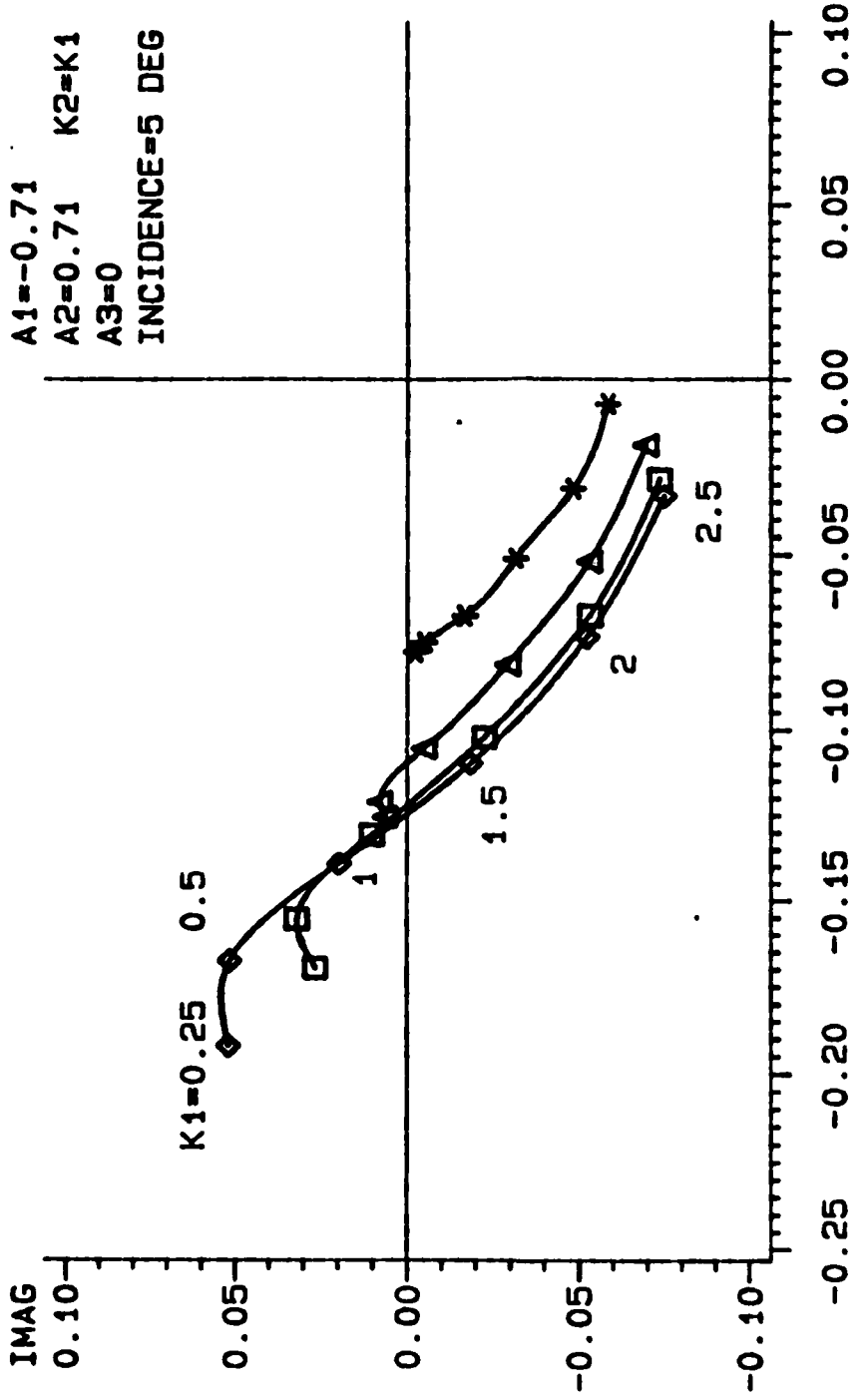

FIGURE 10. THE UNSTEADY MOMENT COEFFICIENT
JOUKOWSKI AIRFOIL: CAMBER=0.05 THICKNESS=0.05

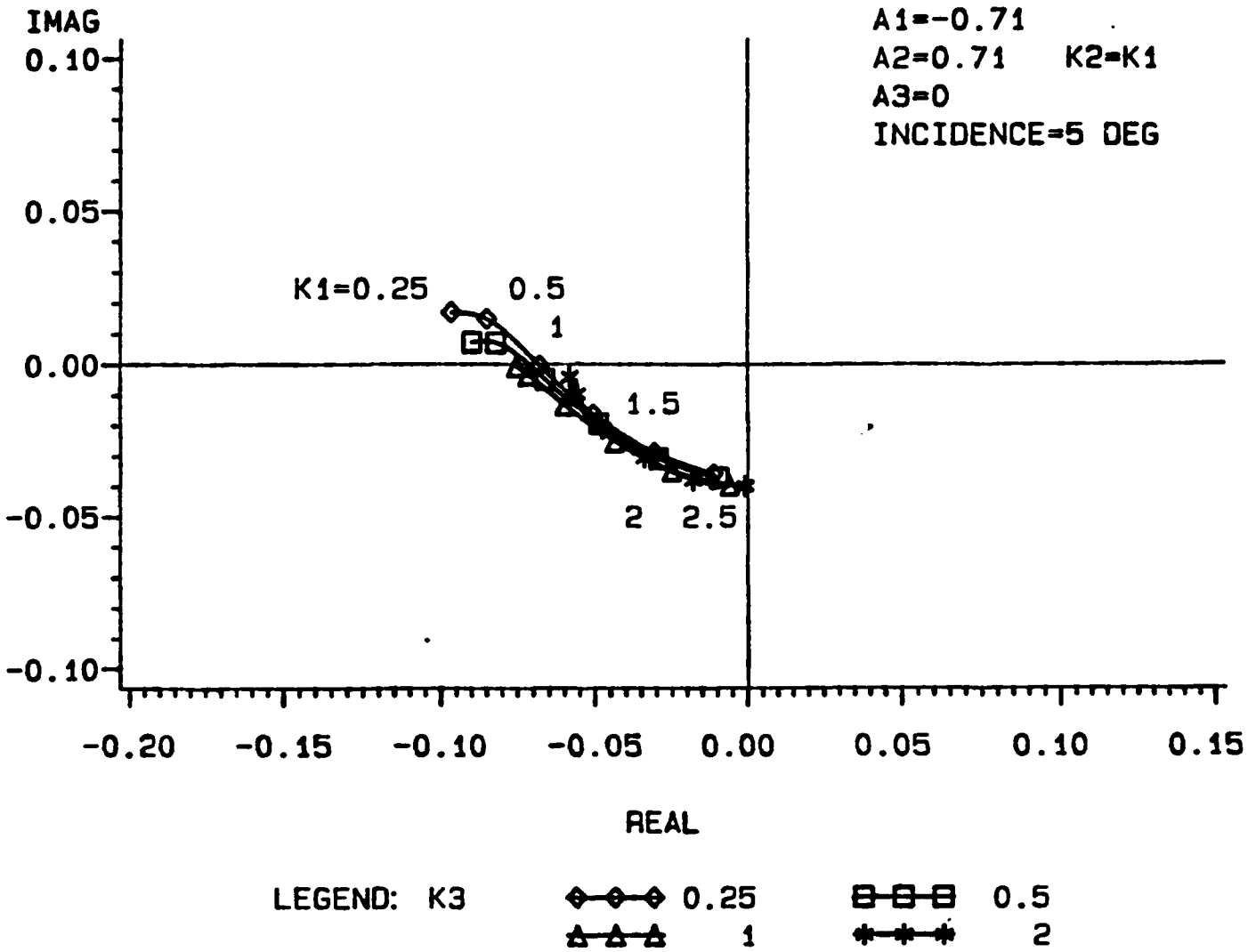

FIGURE 11. THE UNSTEADY DRAG COEFFICIENT
JOUKOWSKI AIRFOIL: CAMBER=0.05 THICKNESS=0.05

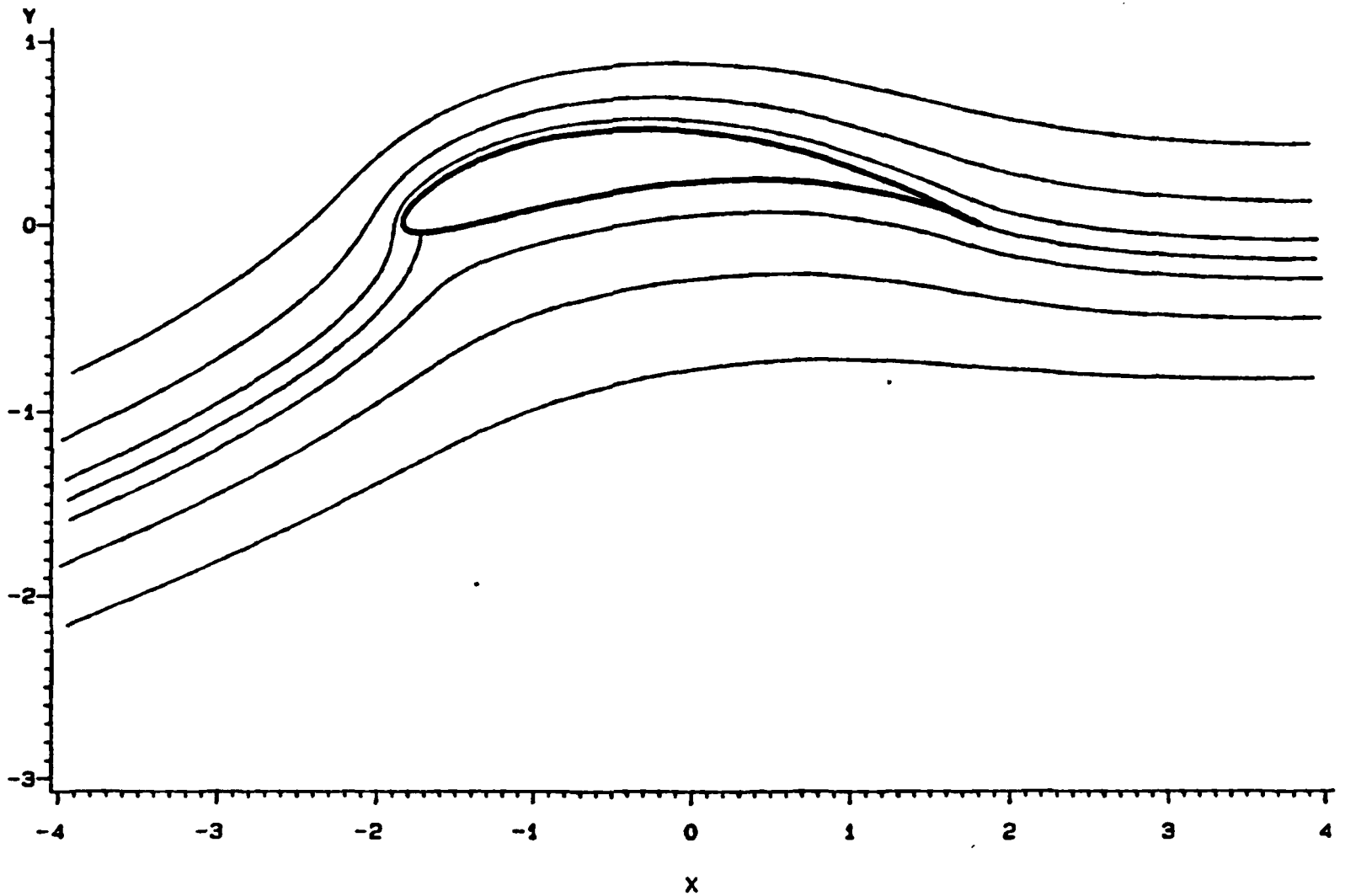

FIGURE 12. JOUKOWSKI AIRFOIL CAMBER=0.1 THICKNESS=0.1 INCIDENCE=10 DEG

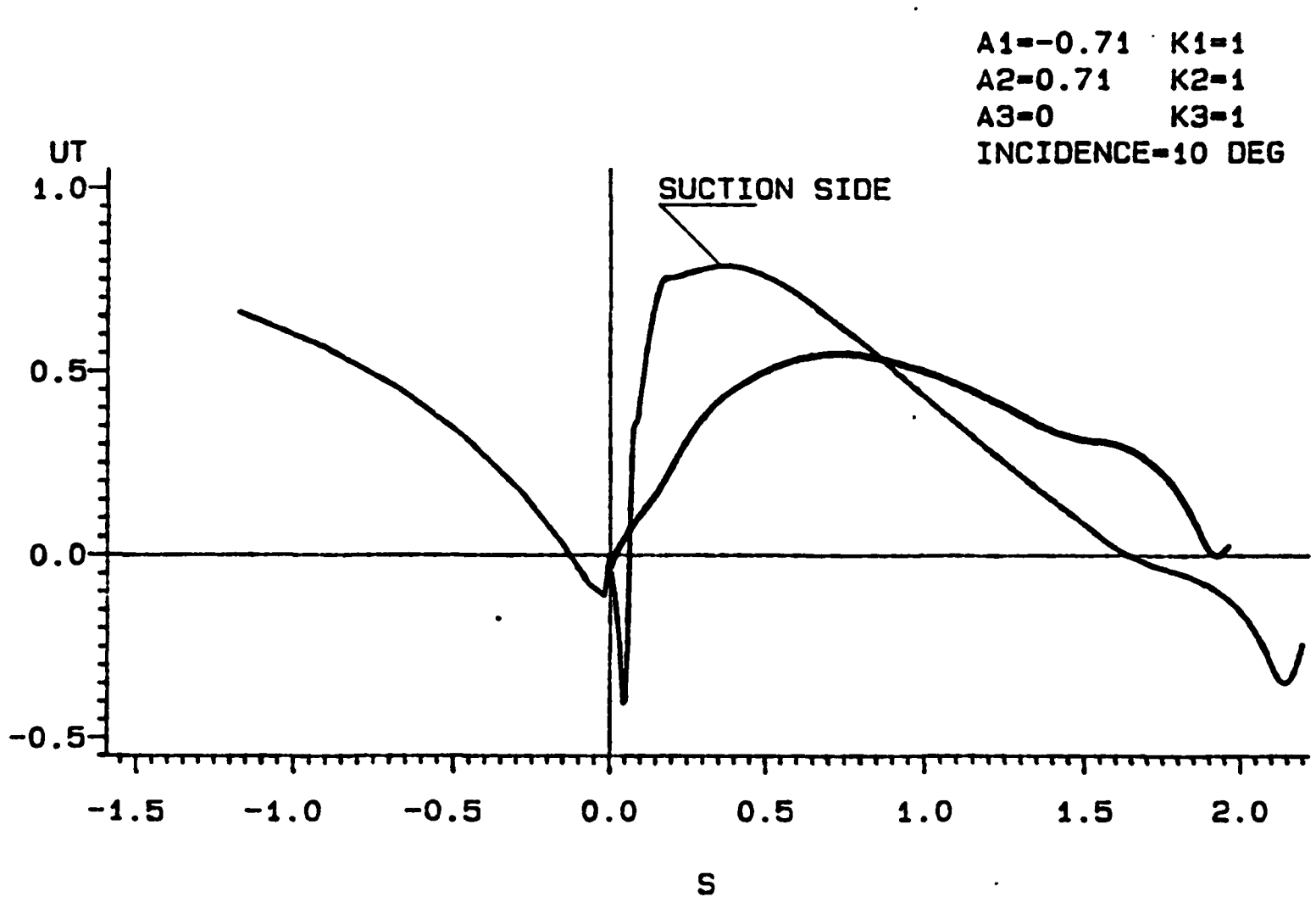

STREAMWISE VELOCITY ALONG THE STAGNATION POINT STREAMLINES (REAL)
JOUKOWSKI AIRFOIL: CAMBER=0.1 THICKNESS=0.1

FIGURE 13.

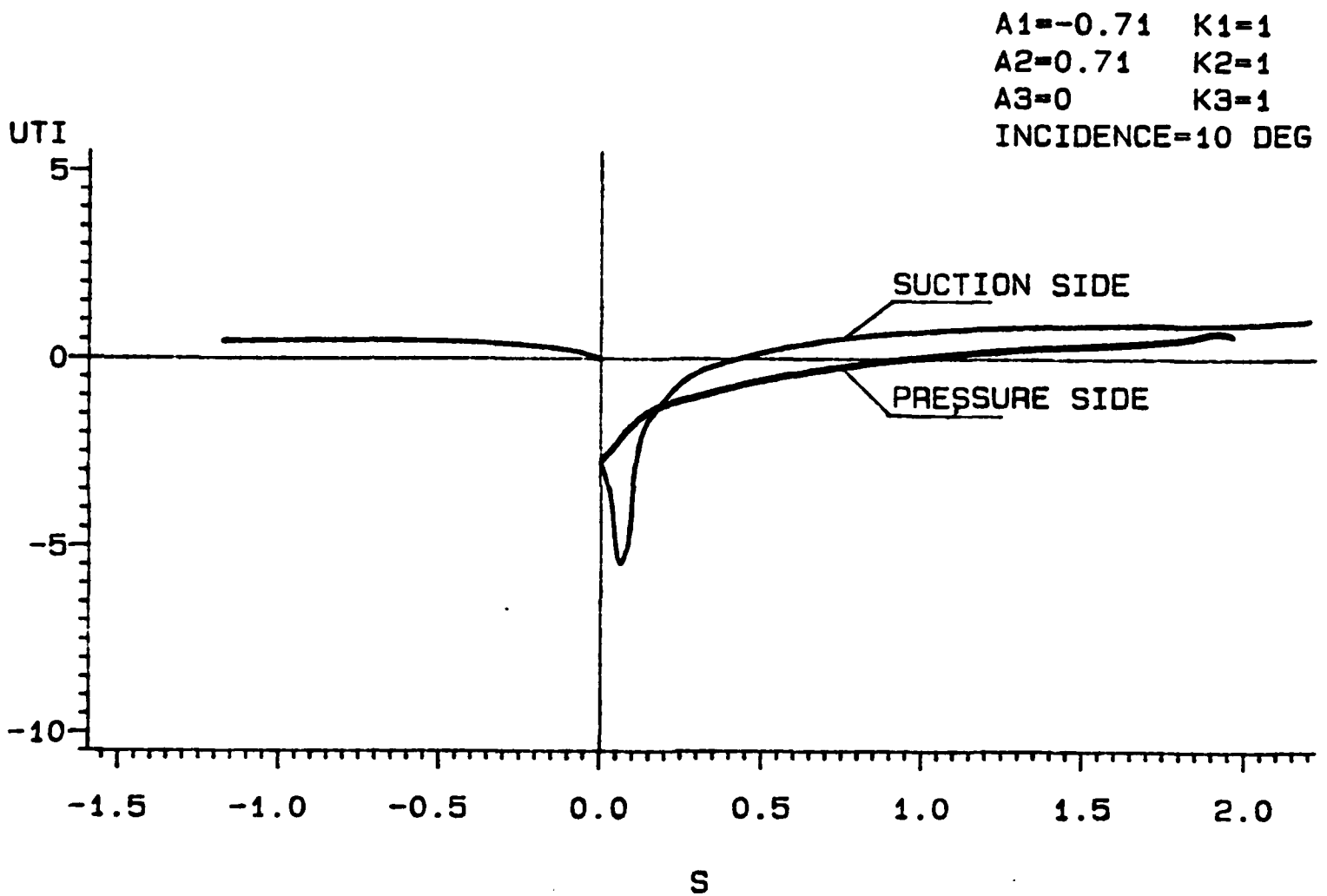

STREAMWISE VELOCITY ALONG THE STAGNATION POINT STREAMLINES (IMAGINARY)
JOUKOWSKI AIRFOIL: CAMBER=0.1 THICKNESS=0.1

FIGURE 14.

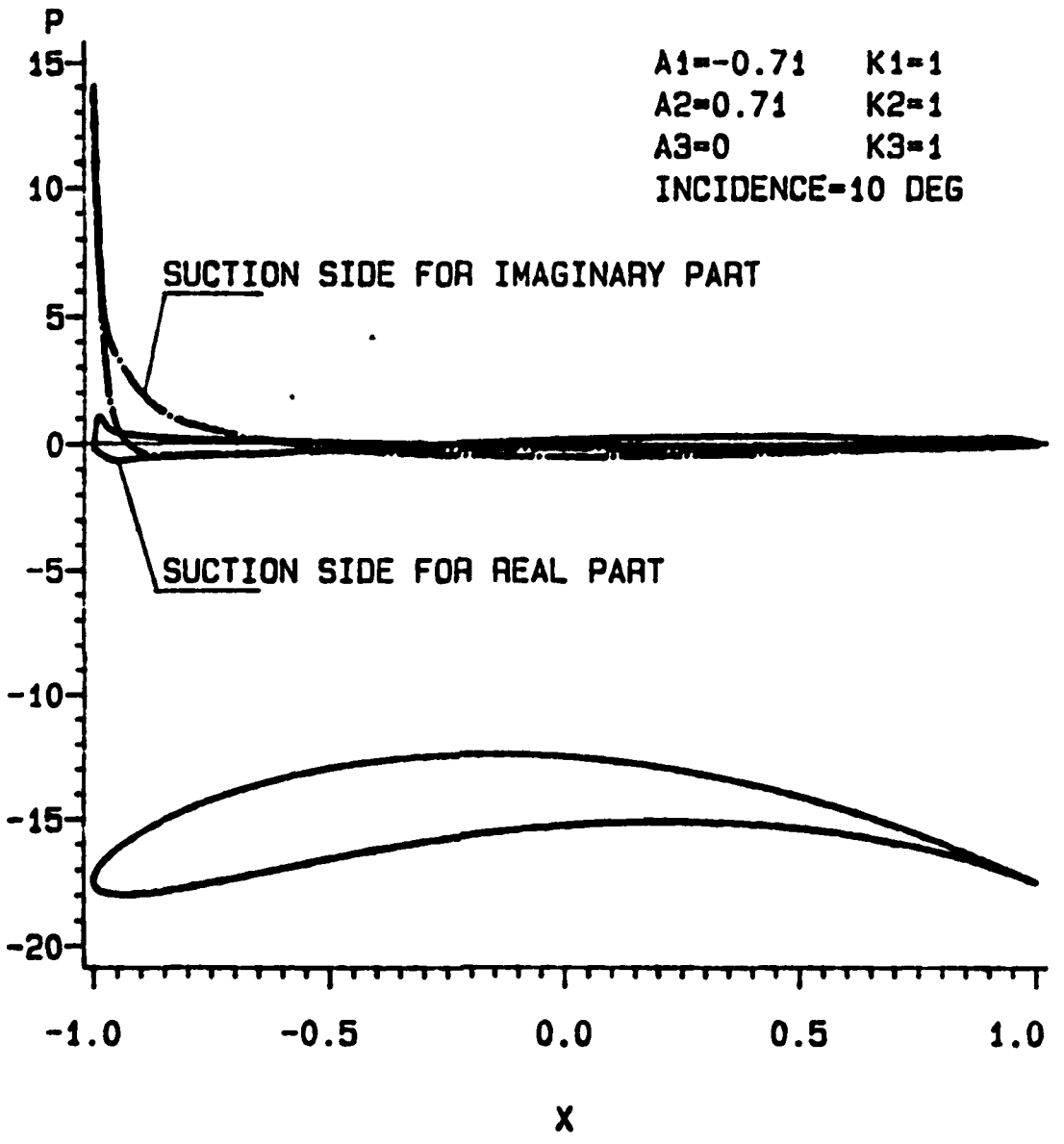

UNSTEADY PRESSURE

FIGURE 15. REAL (SOLID LINE) AND IMAGINARY (DASHED LINE)
JOUKOWSKI AIRFOIL: CAMBER=0.1 THICKNESS=0.1

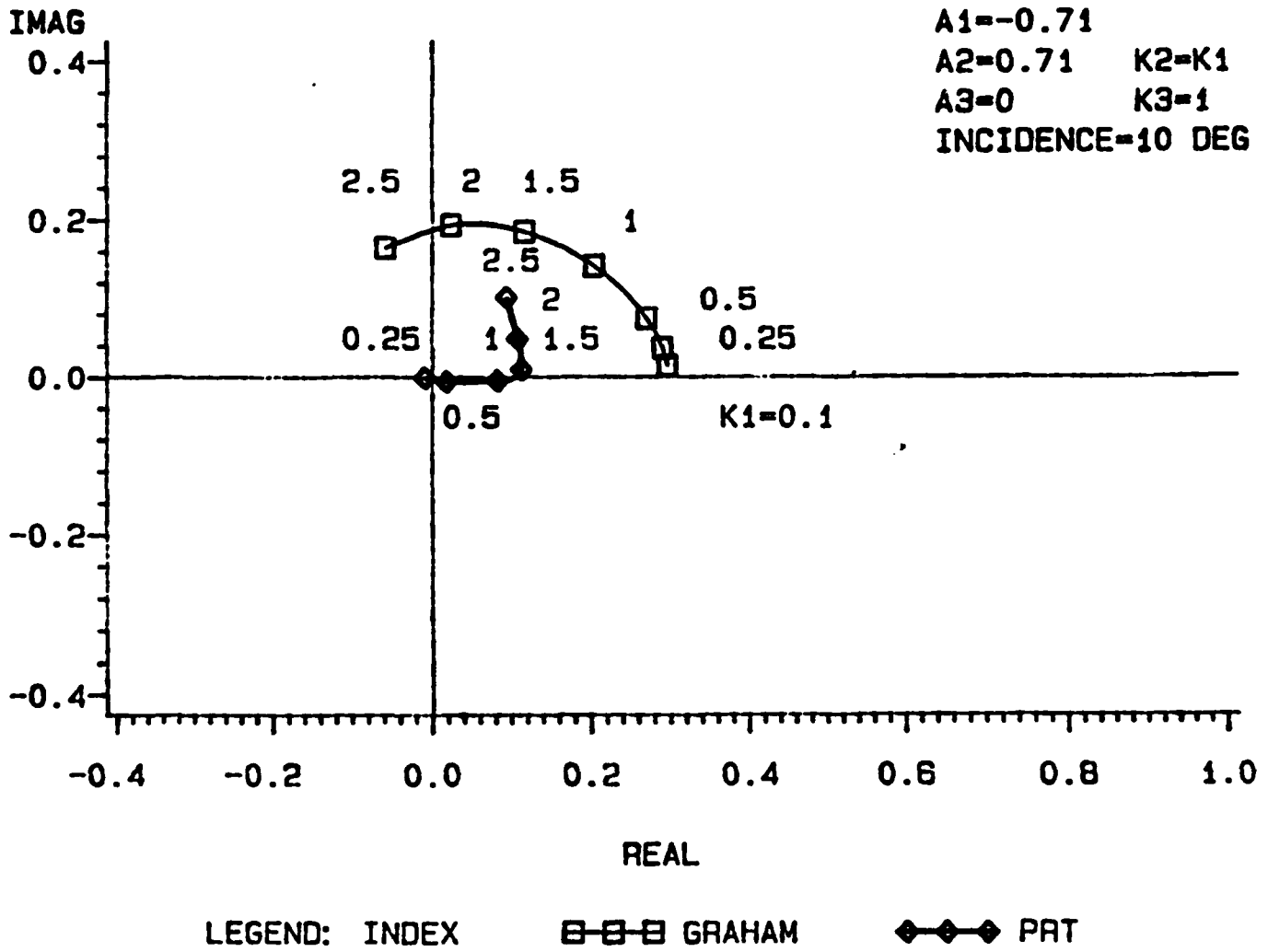

FIGURE 16. THE UNSTEADY LIFT COEFFICIENT
JOUKOWSKI AIRFOIL: CAMBER=0.1 THICKNESS=0.1

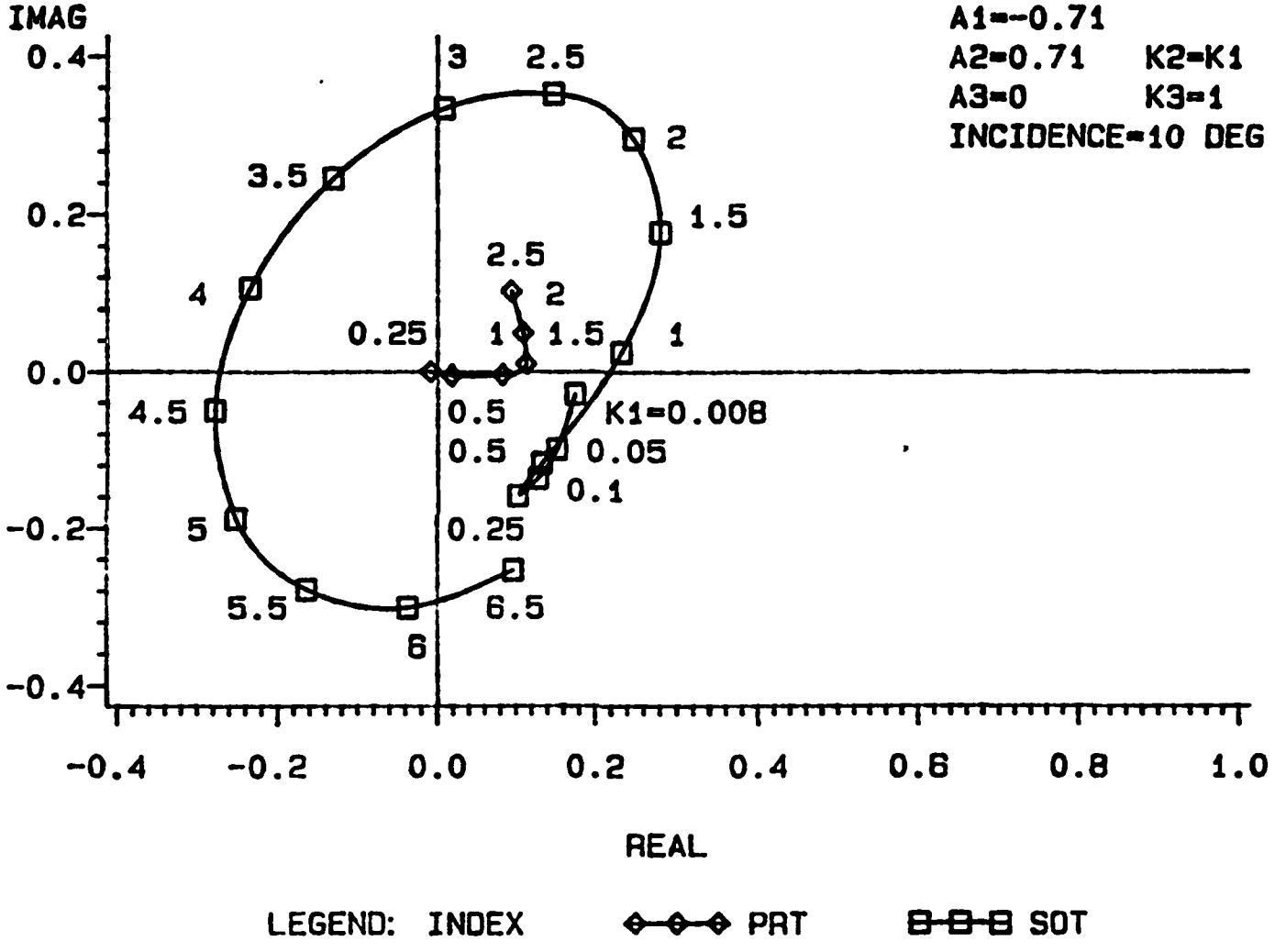

FIGURE 17. THE UNSTEADY LIFT COEFFICIENT
JOUKOWSKI AIRFOIL: CAMBER=0.1 THICKNESS=0.1

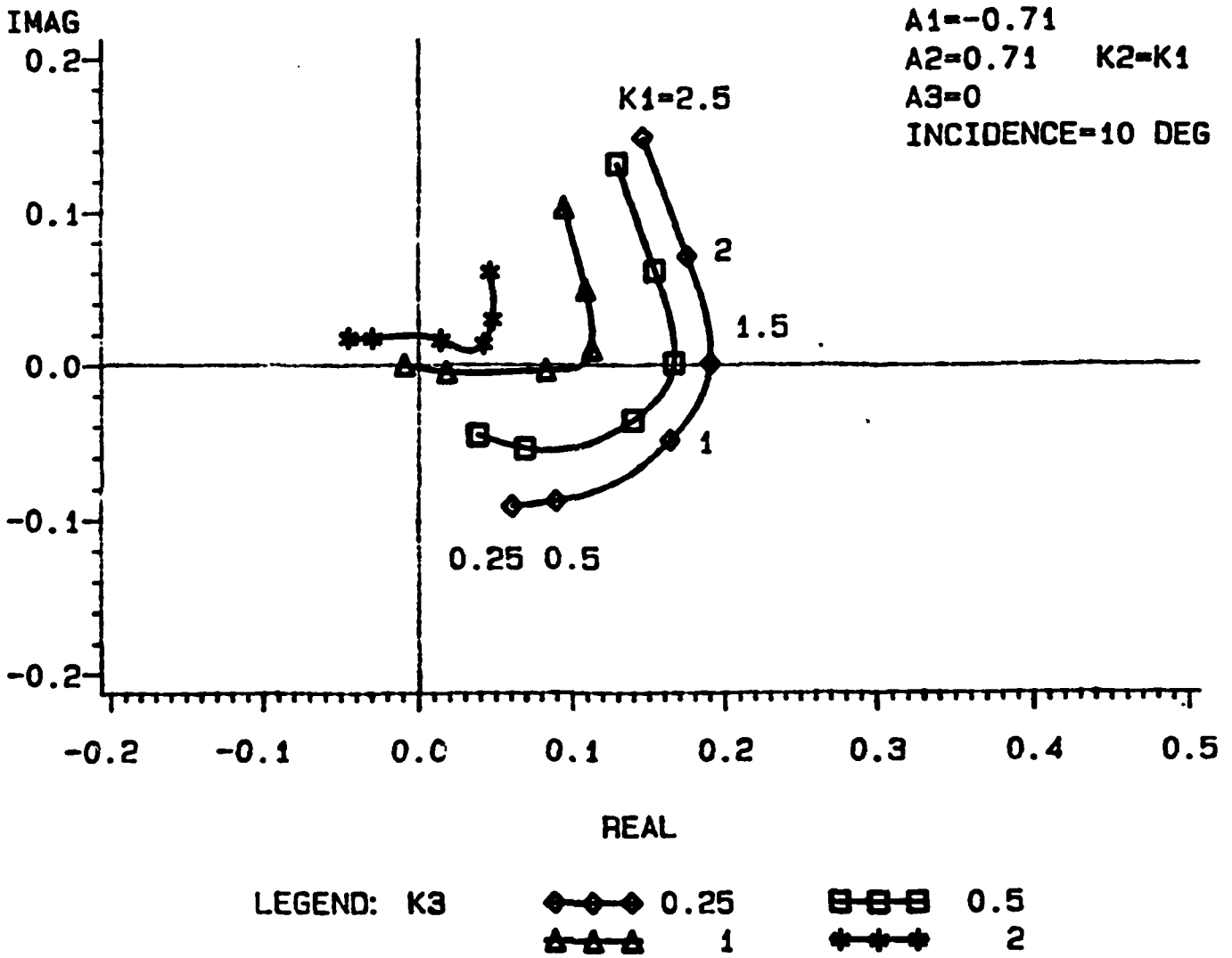

FIGURE 18. THE UNSTEADY LIFT COEFFICIENT
JOUKOWSKI AIRFOIL: CAMBER=0.1 THICKNESS=0.1

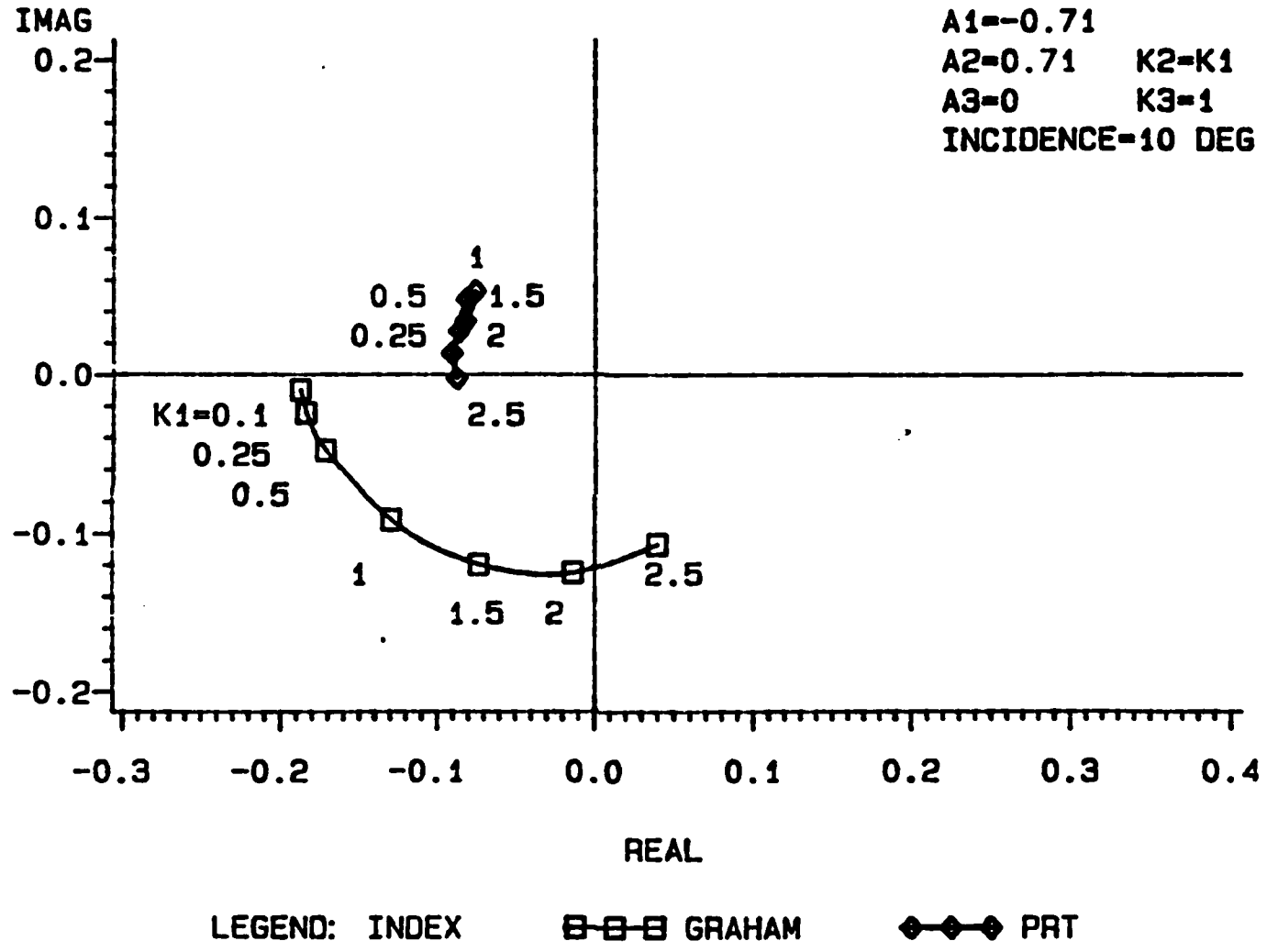

FIGURE 19. THE UNSTEADY MOMENT COEFFICIENT
JOUKOWSKI AIRFOIL: CAMBER=0.1 THICKNESS=0.1

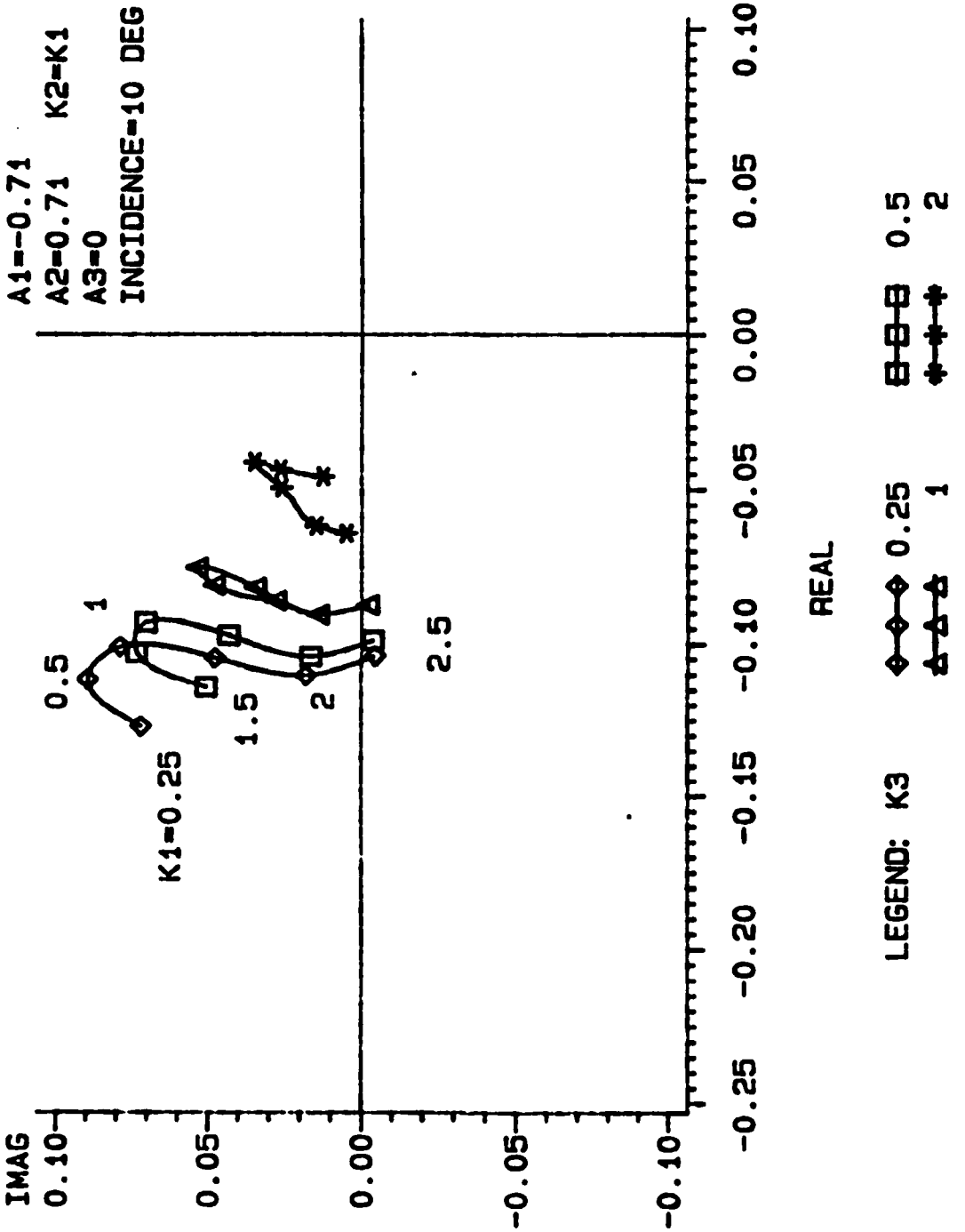

FIGURE 20. THE UNSTEADY MOMENT COEFFICIENT
JOUKOWSKI AIRFOIL: CAMBER=0.1 THICKNESS=0.1

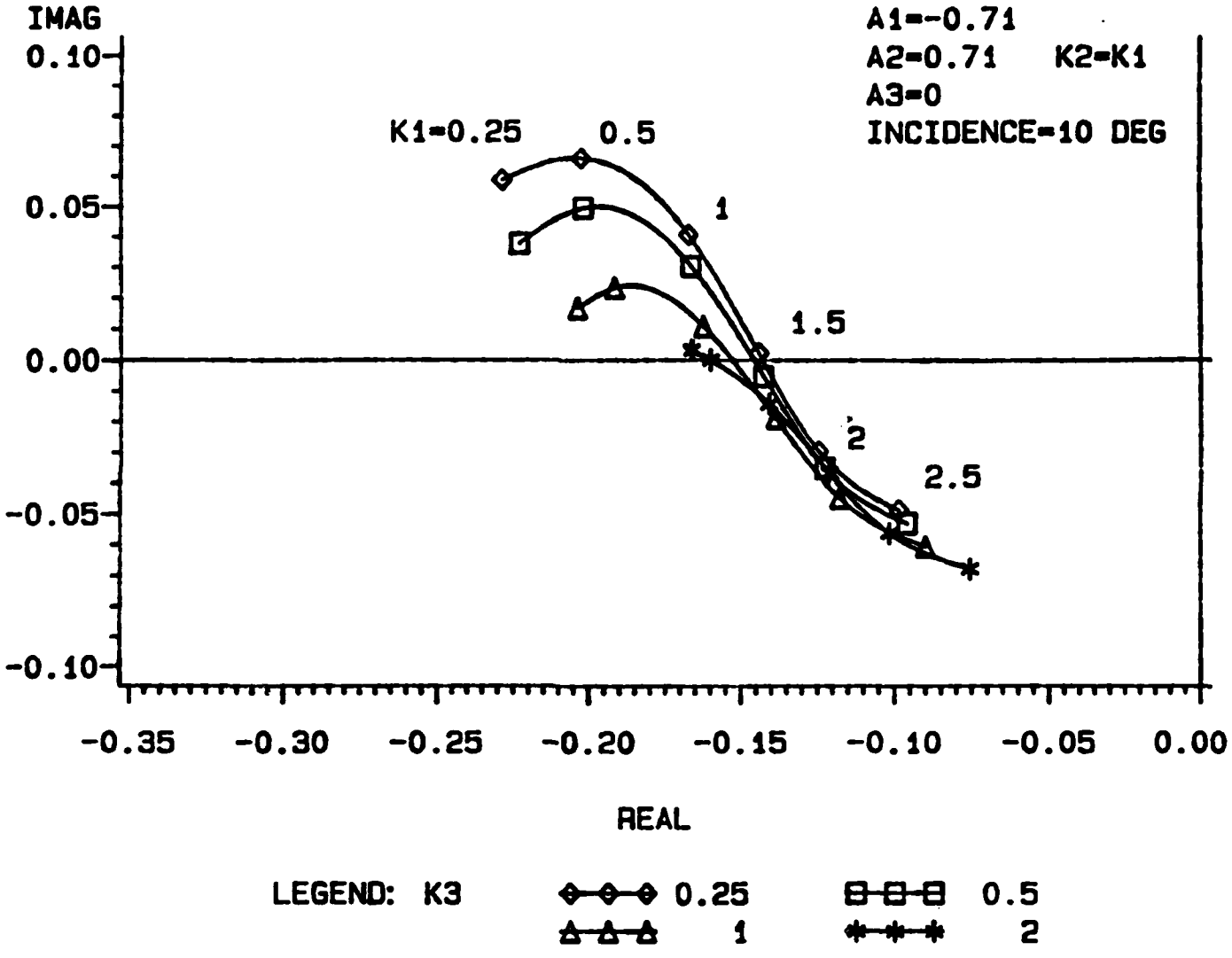

FIGURE 21. THE UNSTEADY DRAG COEFFICIENT
JOUKOWSKI AIRFOIL: CAMBER=0.1 THICKNESS=0.1

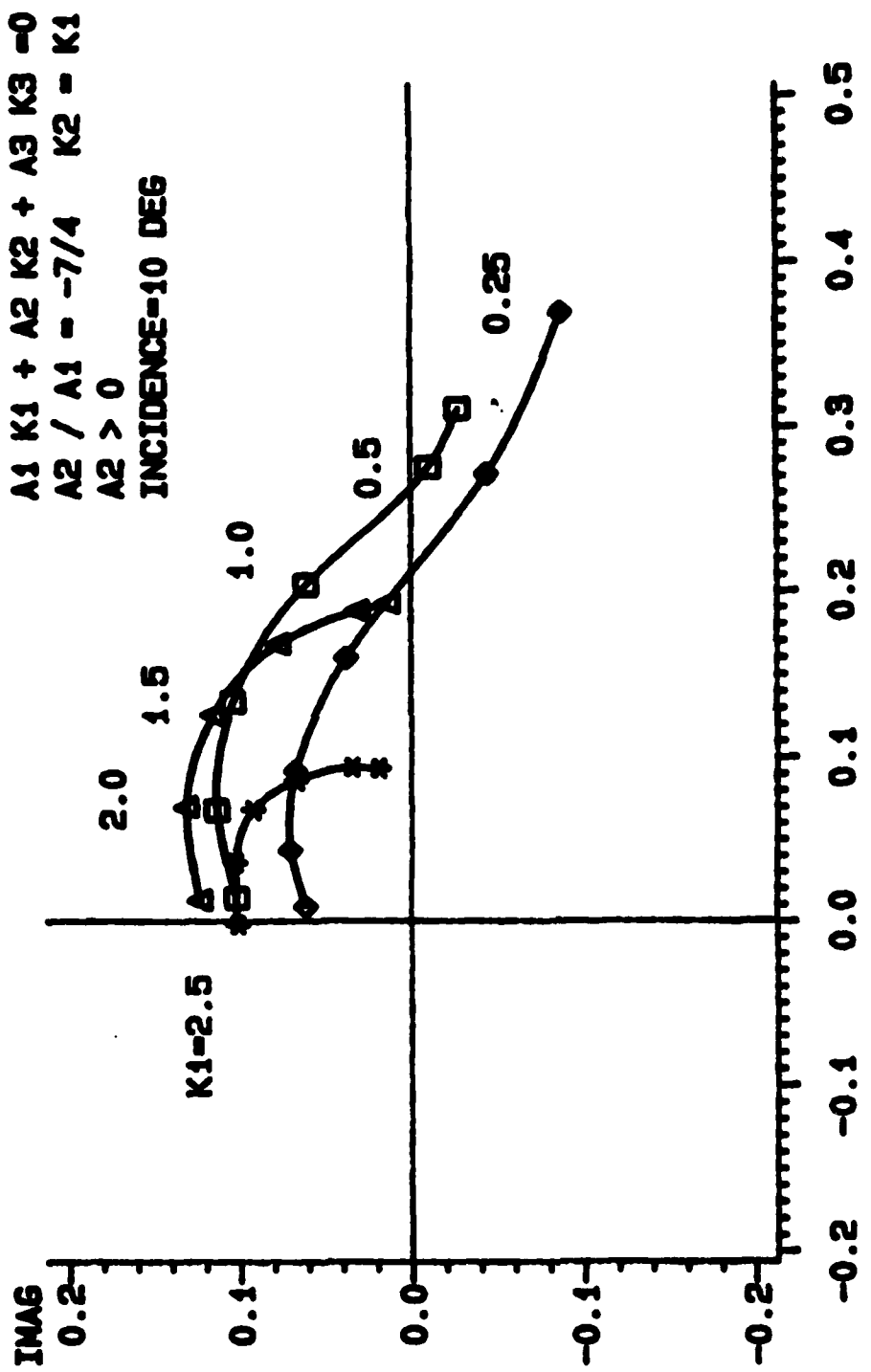

FIGURE 22. THE UNSTEADY LIFT COEFFICIENT
JOUKOWSKI AIRFOIL: CAMBER=0.1 THICKNESS=0.1

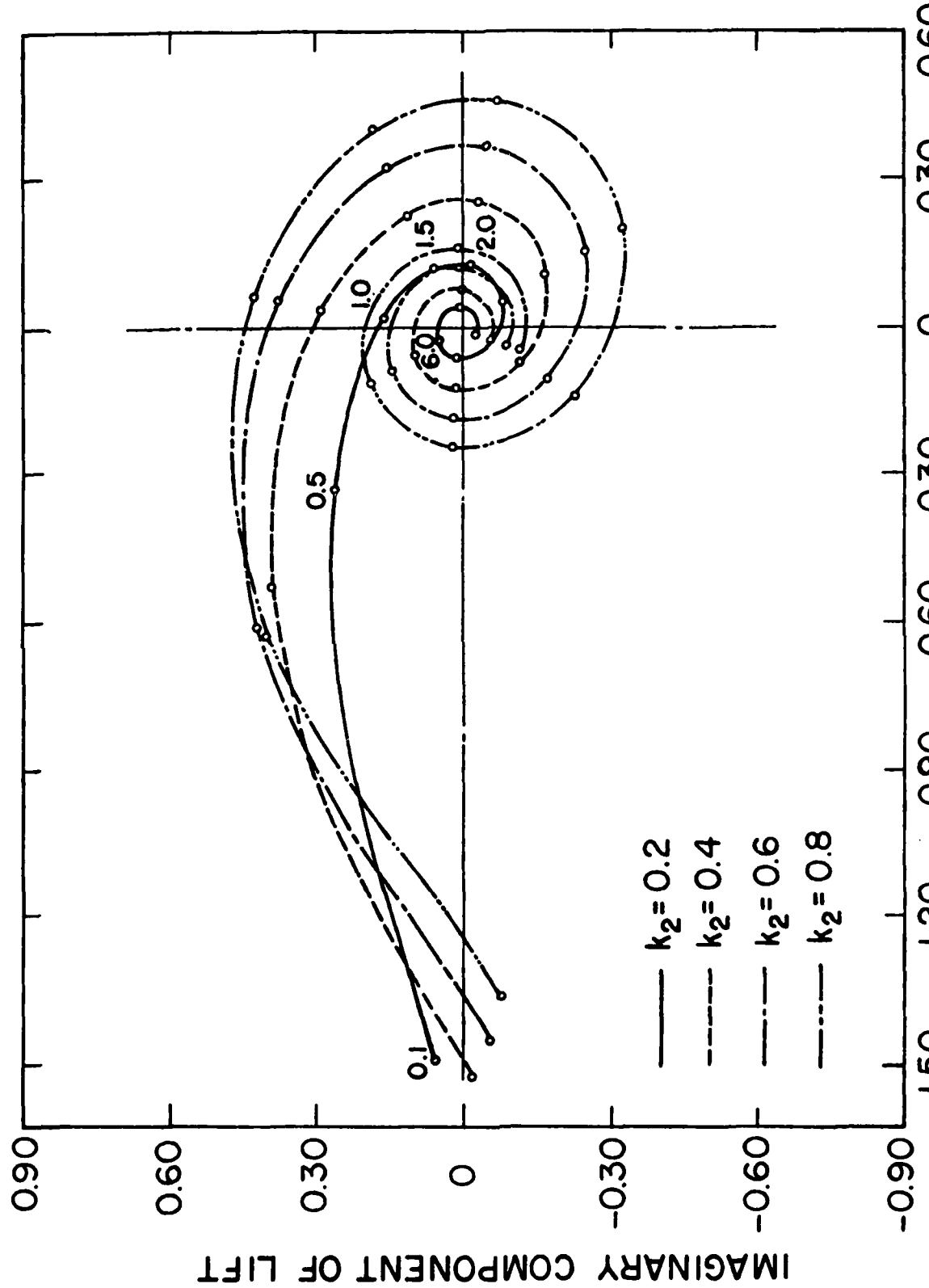

FIGURE 23. VECTOR DIAGRAM SHOWING THE REAL AND IMAGINARY PARTS OF THE RESPONSE FUNCTION R_6 VERSUS THE REDUCED FREQUENCY k_1

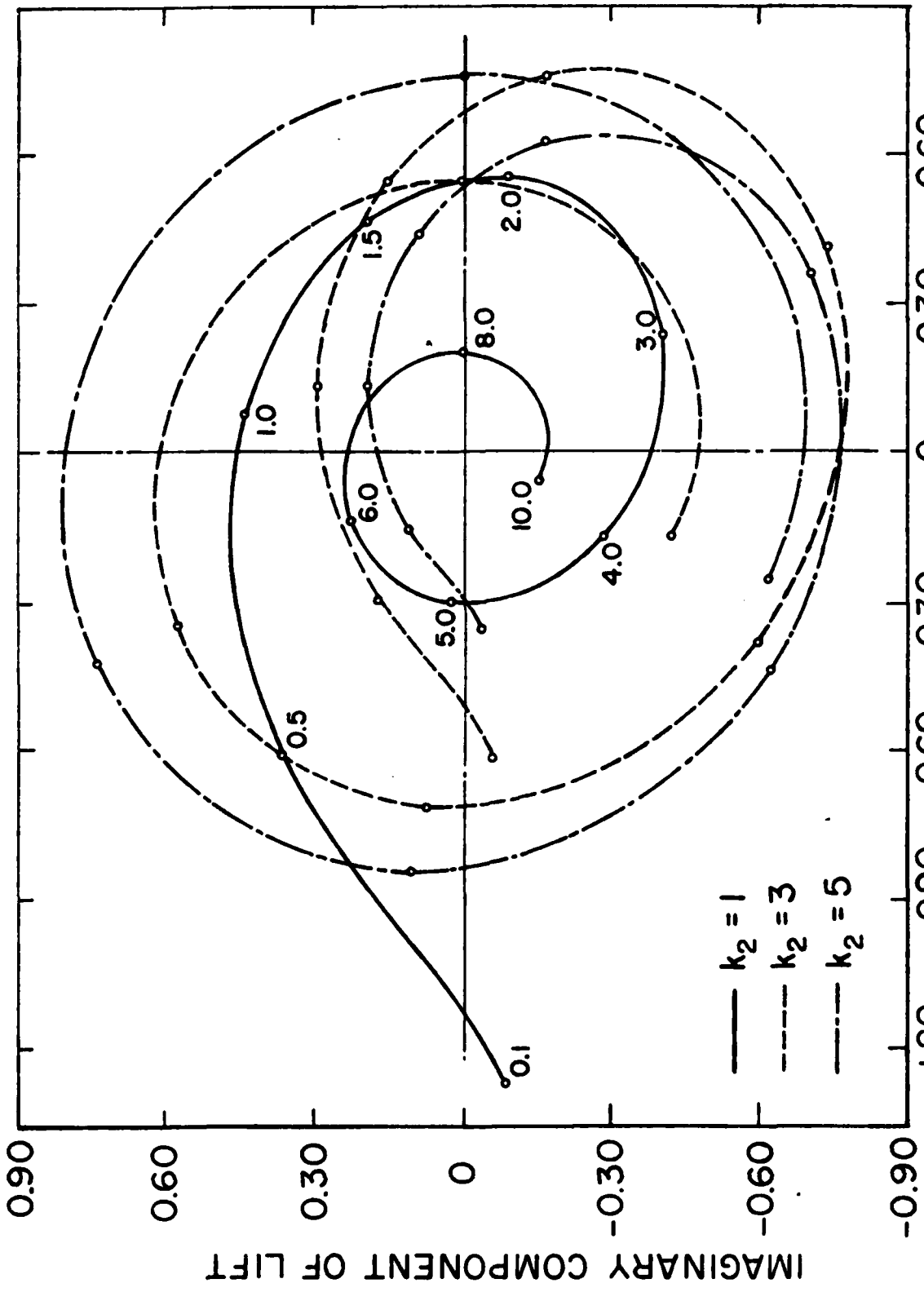

FIGURE 24. VECTOR DIAGRAM SHOWING THE REAL AND IMAGINARY PARTS OF THE RESPONSE FUNCTION R_β VERSUS THE REDUCED FREQUENCY k_1

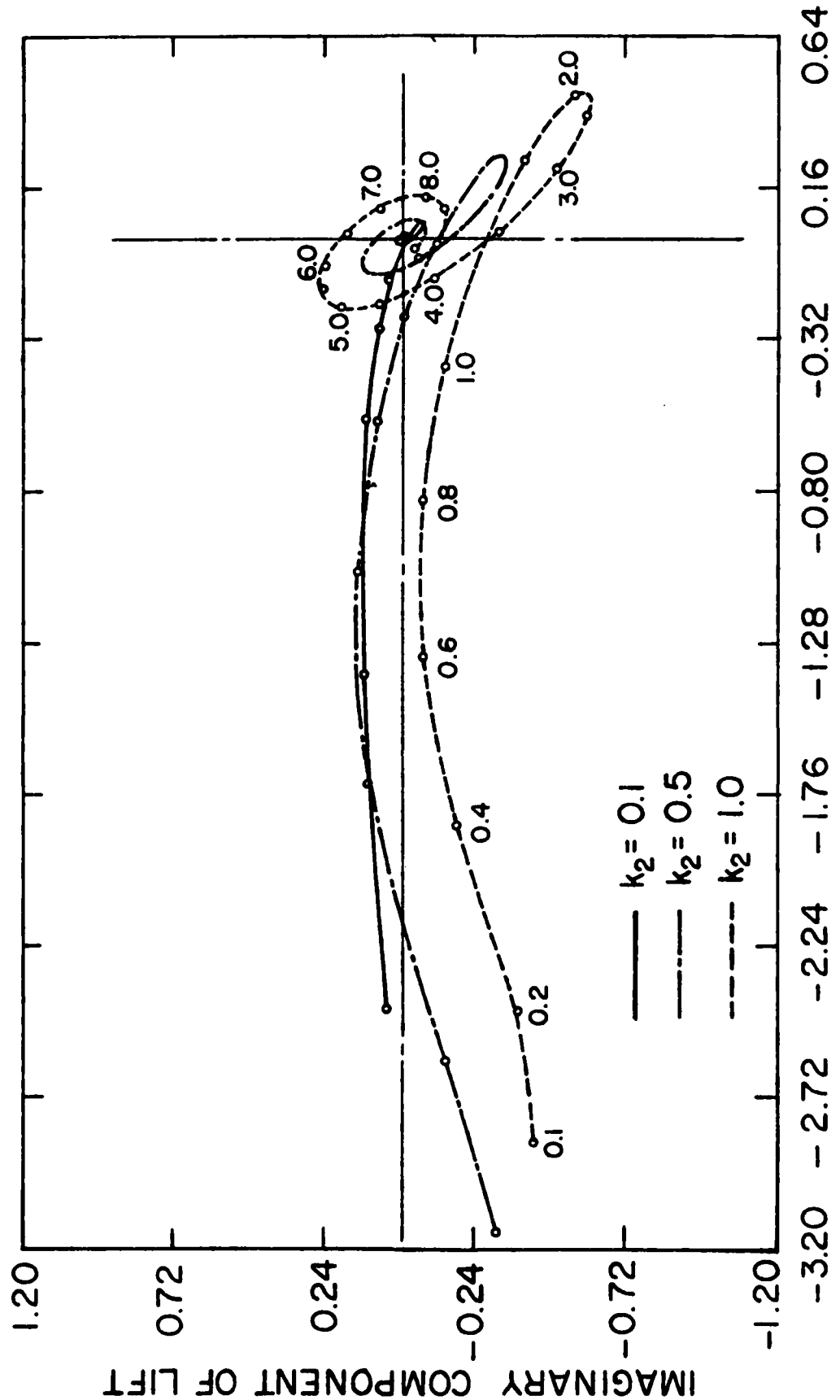

FIGURE 25. VECTOR DIAGRAM SHOWING THE REAL AND IMAGINARY PARTS OF R_m VERSUS THE REDUCED FREQUENCY k_1

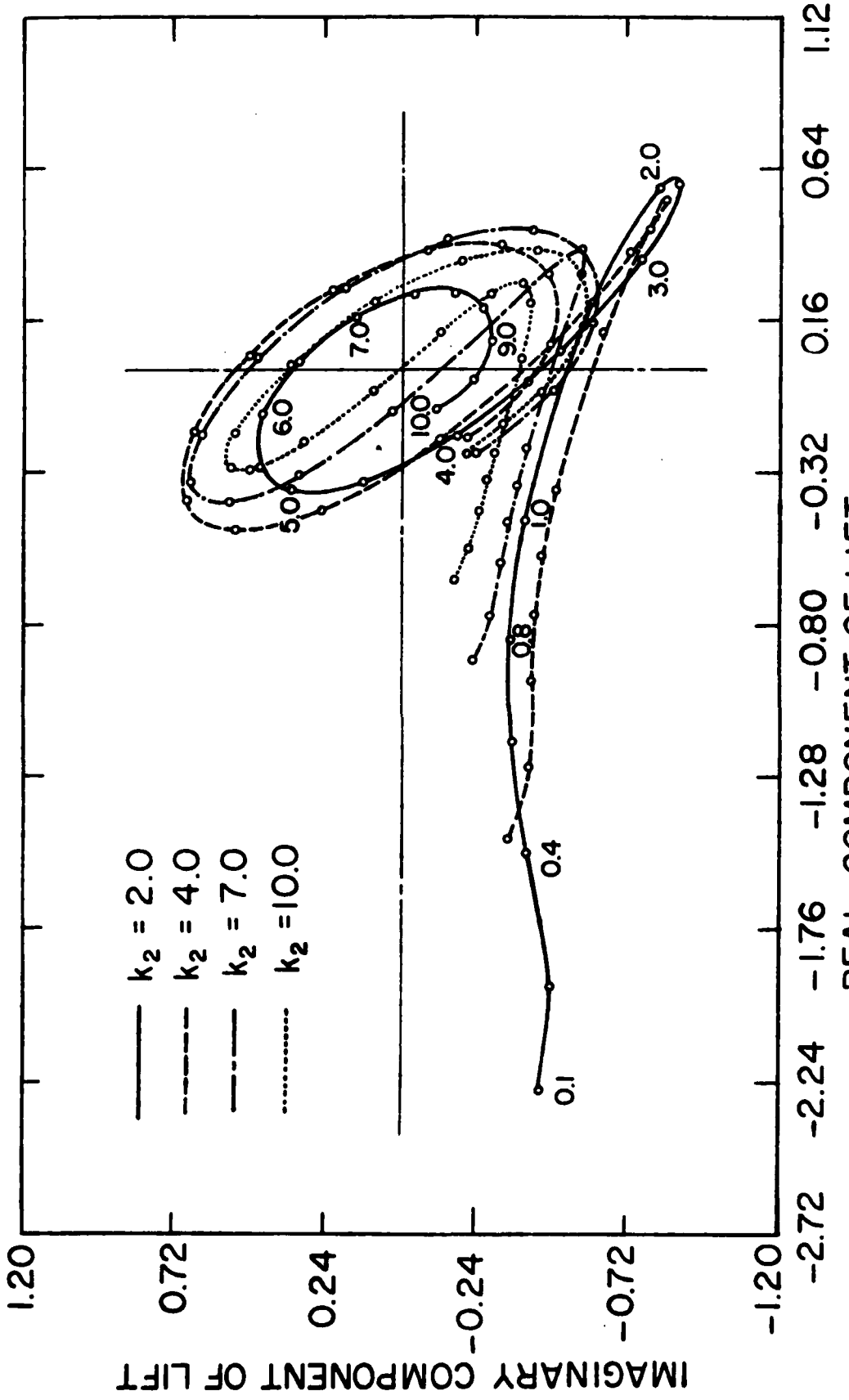

FIGURE 26. VECTOR DIAGRAM SHOWING THE REAL AND IMAGINARY PARTS OF R_m VERSUS THE REDUCED FREQUENCY k_1

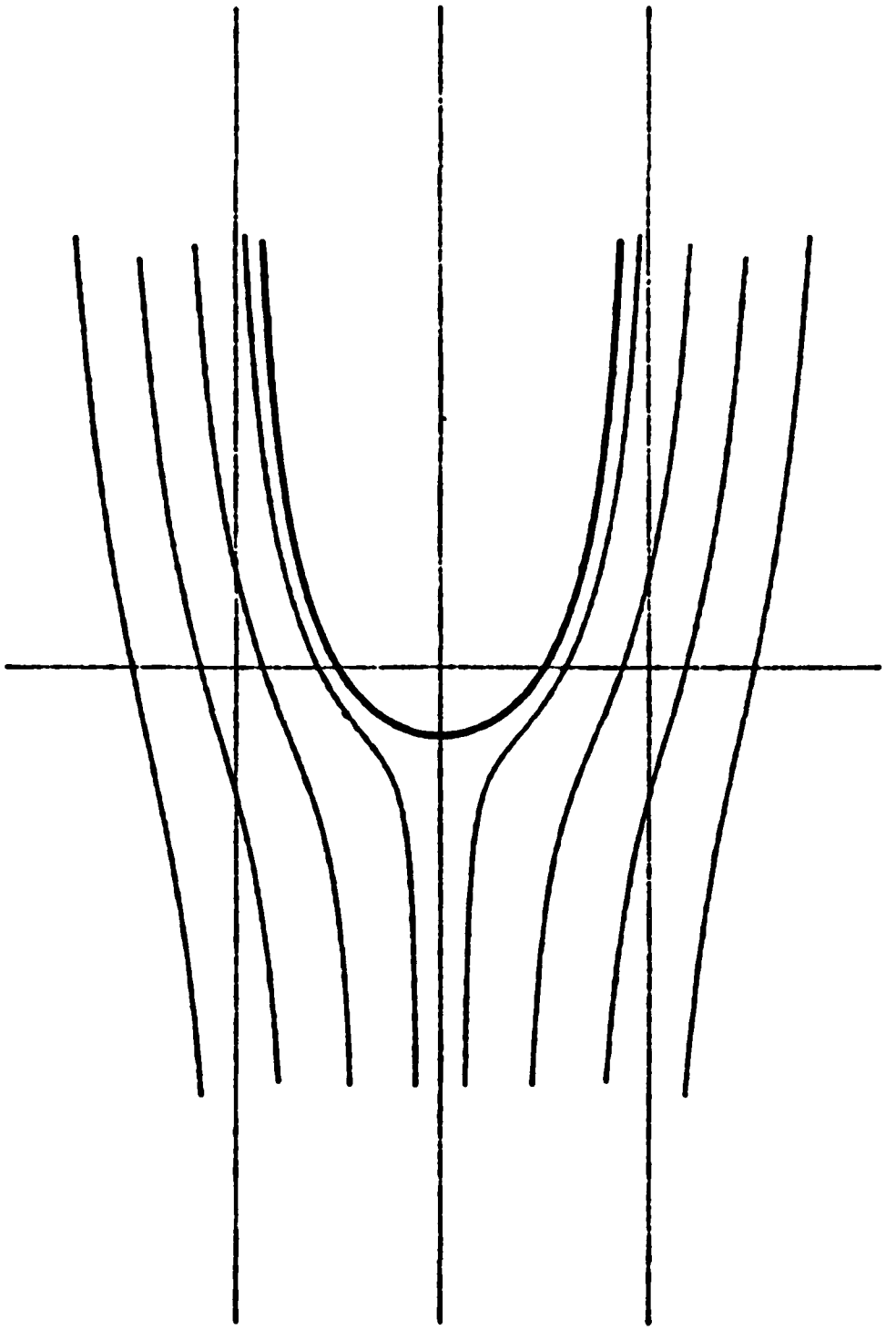

FIGURE 27. STEADY FLOW STREAMLINES

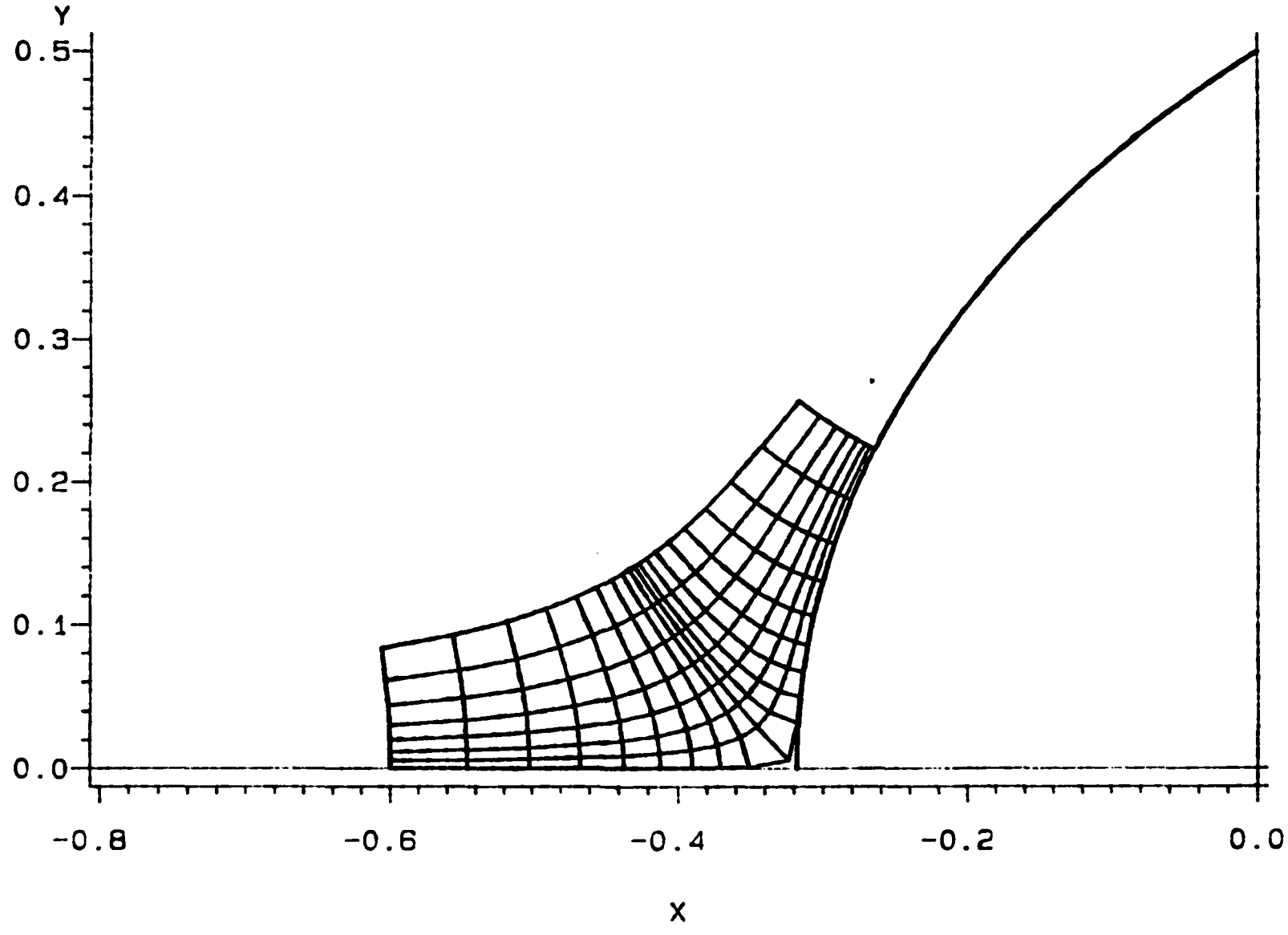

FIGURE 28. THE STEADY FLOW AROUND THE BLUFF BODY STAGNATION POINT

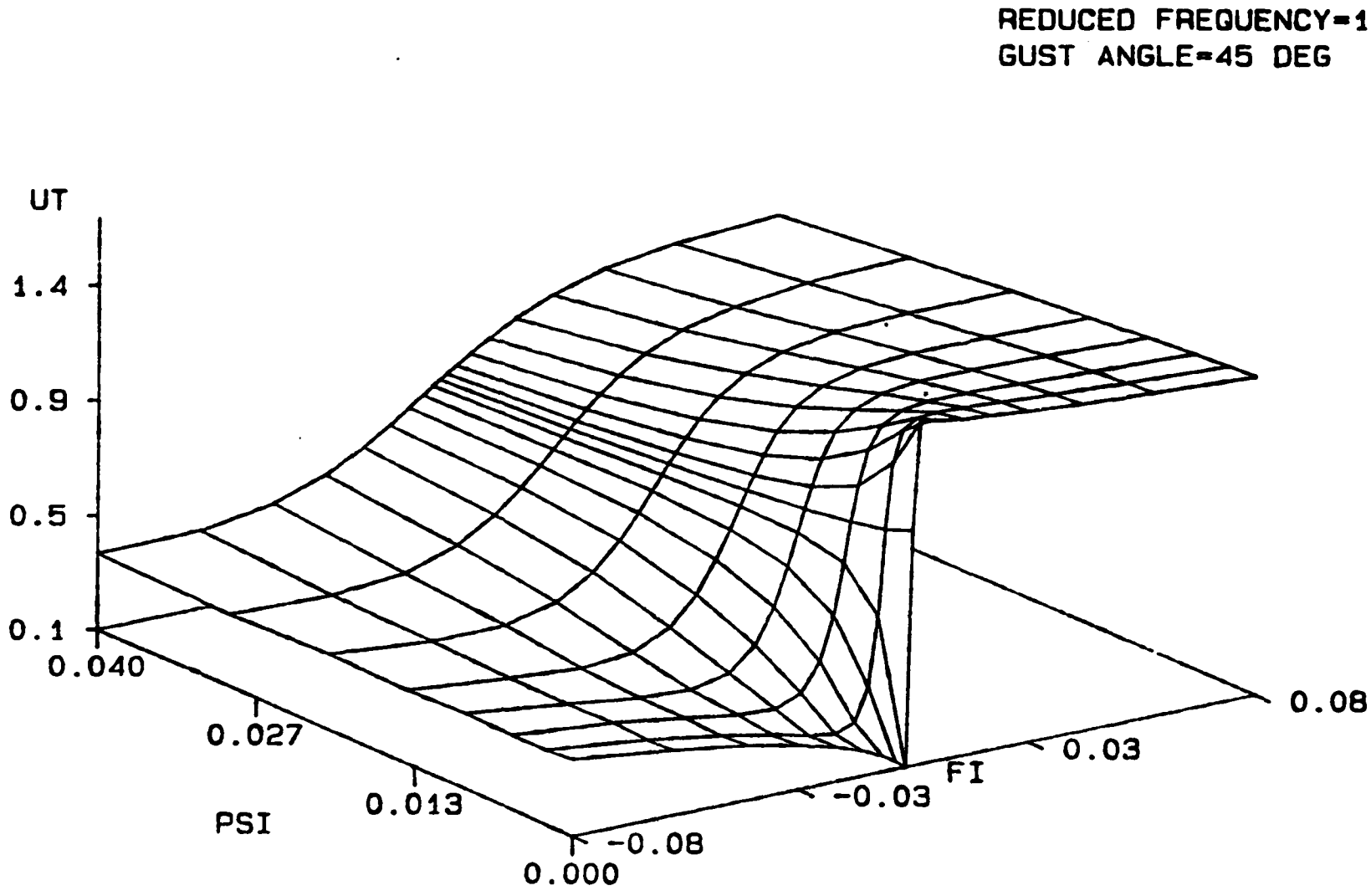

FIGURE 29. THE MAGNITUDE OF THE STREAMWISE VELOCITY
BLUFF BODY (U=1 M=U/PI)

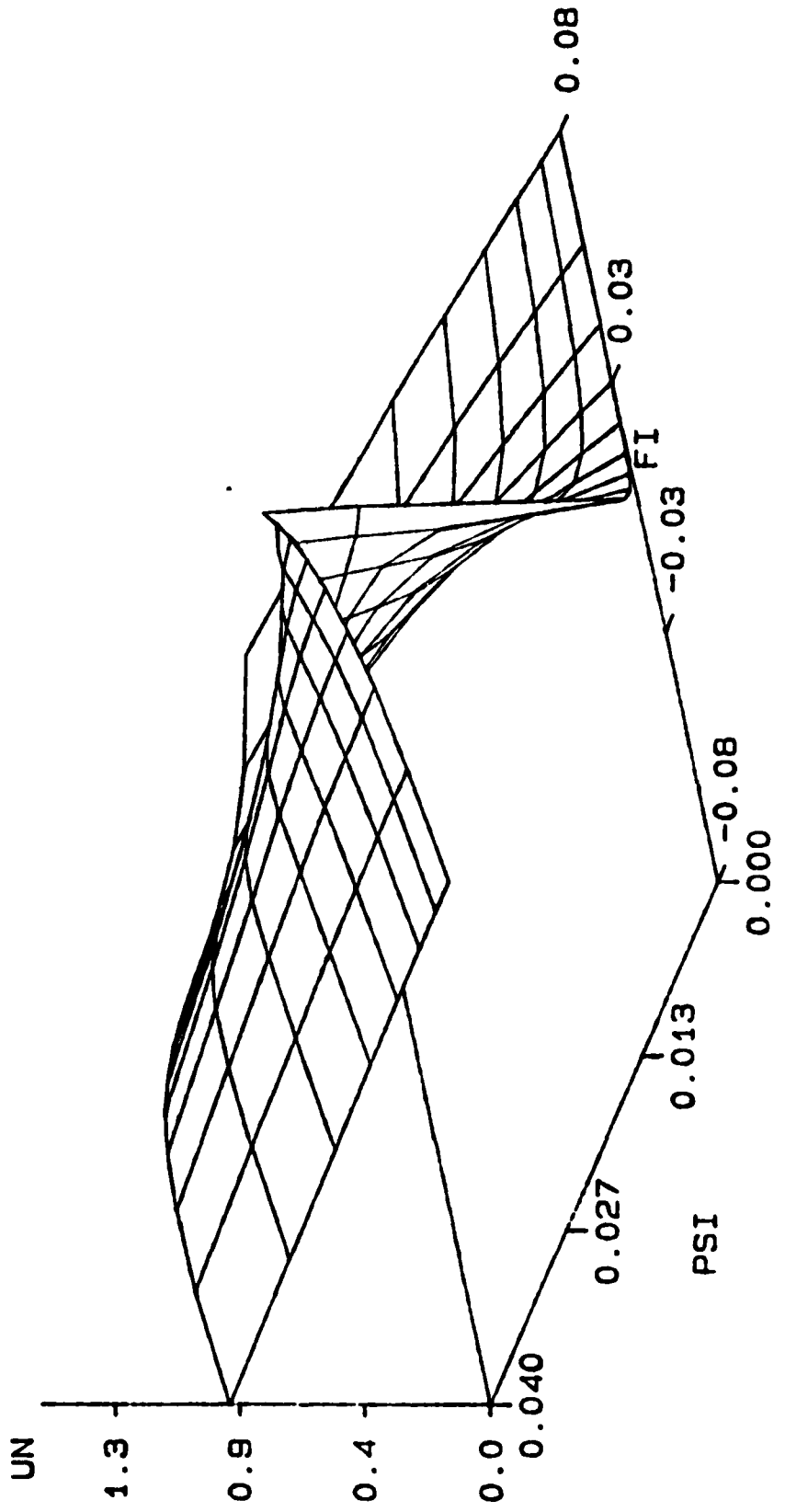

FIGURE 30. THE MAGNITUDE OF THE NORMAL VELOCITY
BLUFF BODY (U=1 M=U/PI)

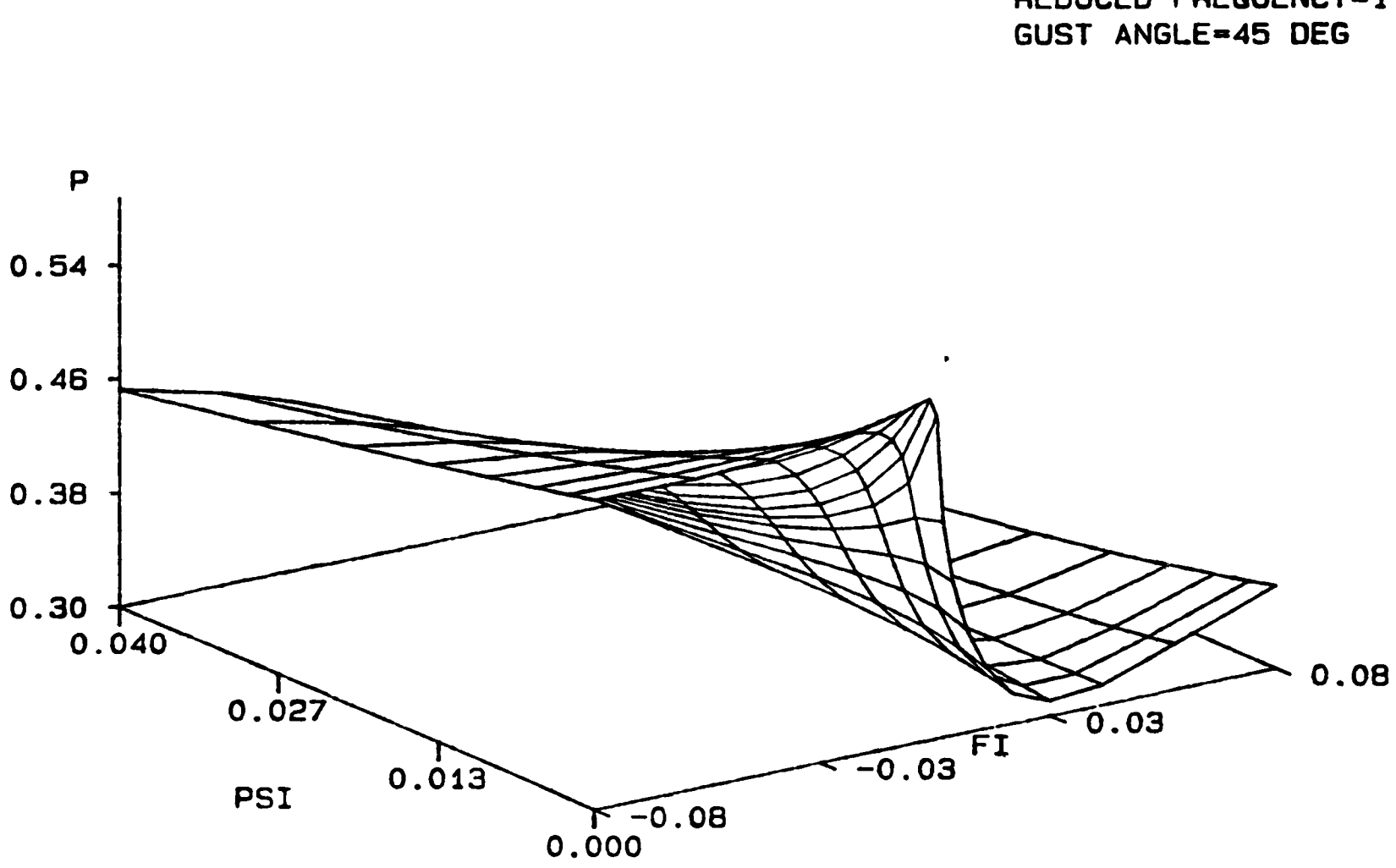

FIGURE 31. THE MAGNITUDE OF THE UNSTEADY PRESSURE
BLUFF BODY (U=1 M=U/PI)

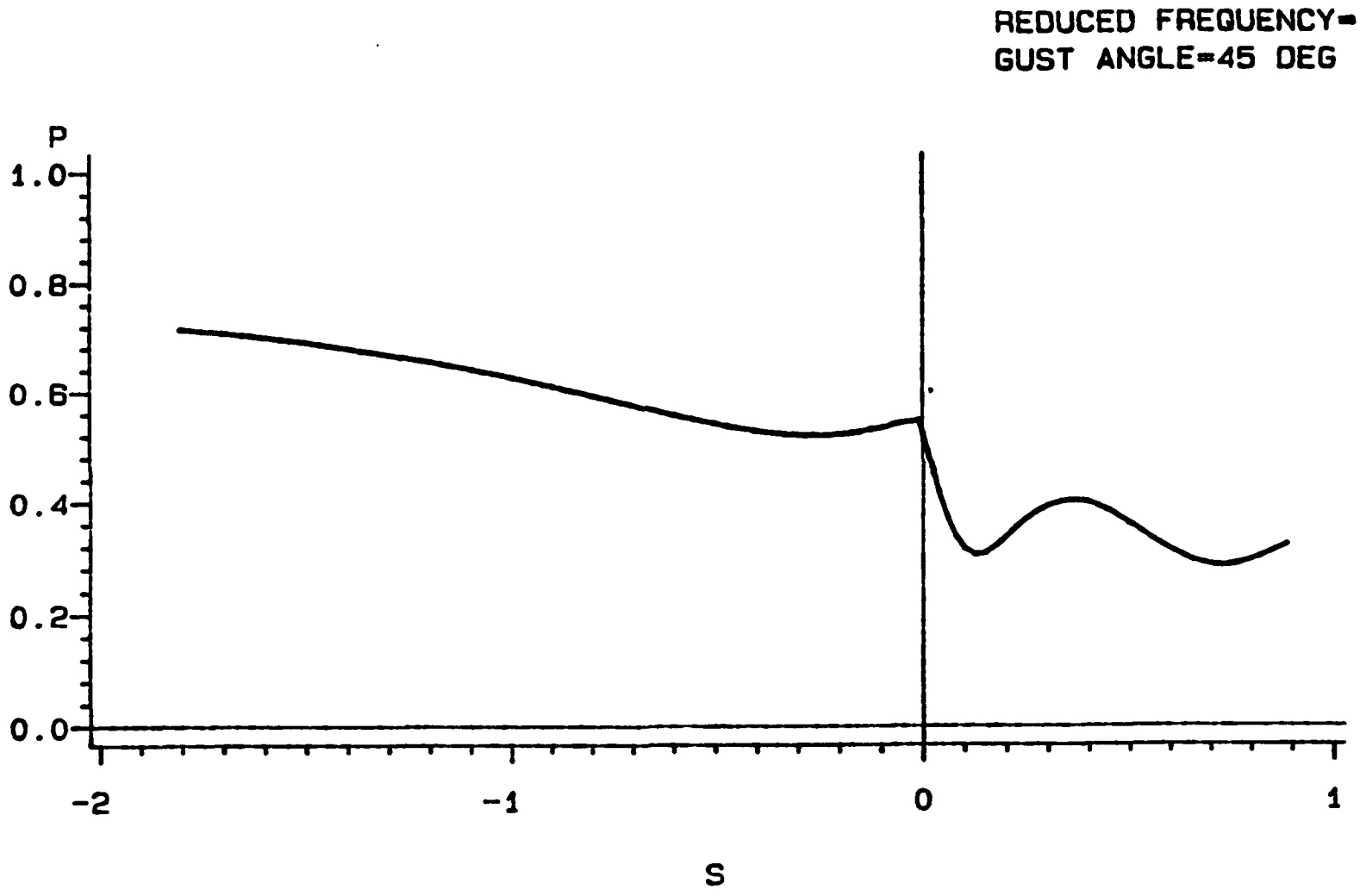

FIGURE 32. THE MAGNITUDE OF THE UNSTEADY PRESSURE ALONG THE STREAMLINE PSI=0 BLUFF BODY (U=1 M=U/PI)

VIII. PUBLICATIONS RESULTING FROM OUR WORK UNDER AFOSR SPONSORSHIP

All publications listed below are authored by Professor Atassi. Only co-authors are listed.

"Regularization of Goldstein's Splitting of Unsteady Vortical and Entropic Distortions of Potential Flows," Invited Paper, 19th Annual Meeting, Society of Engineering Science, Rolla, Missouri, P. 354, October 1982.

"Unsteady Vortical Distortions of Potential Flows Round Bluff Bodies," co-author, J. Grzedzinski, Bull. Amer. Phys. Soc., Vol. 24, No. 8, p. 1356, November 1983.

"The Sears' Problem for a Lifting Airfoil Revisited - New Results," Journal of Fluid Mechanics, Vol. 141, pp. 109-122, 1984.

"A Uniformly Valid Splitting of Unsteady Vortical and Entropic Disturbances of Potential Flows," to be submitted to Journal of Fluid Mechanics.

"Three-Dimensional Periodic Vortical Disturbances Acting Upon an Airfoil," to be submitted to Journal of Fluid Mechanics. Co-author J. Grzedzinski.

IX. PERSONNEL

All people who worked under the present grant are listed below:

Hafiz Atassi, Professor and Principal Investigator

John Grzedzinski, Research Assistant

Albin A. Szewczyk, Professor (partial support)

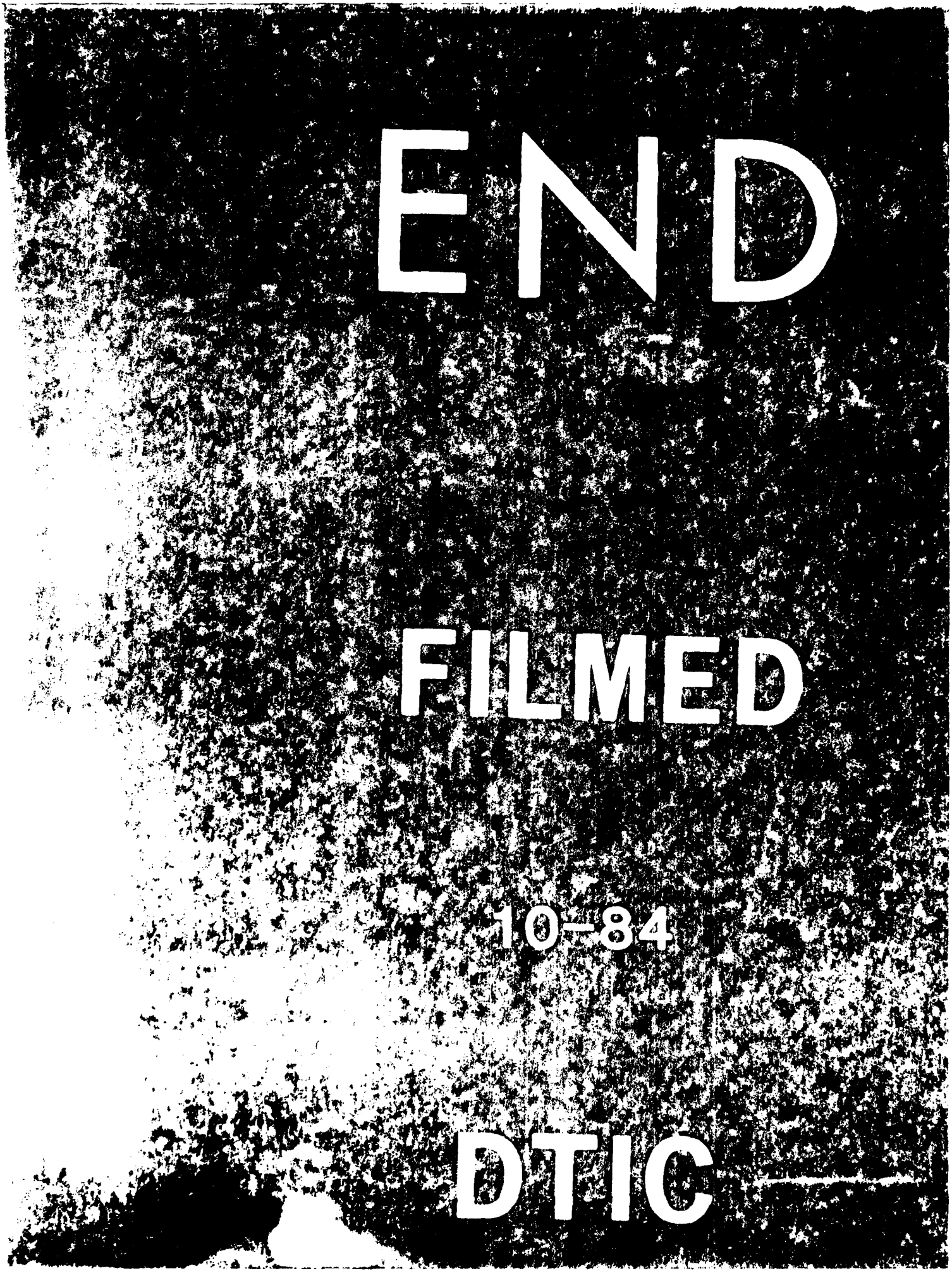
END
FILMED
10-84
DTIC